Angewandte Chemie
Eine Zeitschrift der Gesellschaft Deutscher Chemiker

Supporting Information

A Heterogeneous Palladium Catalyst for the Polymerization of Olefins Prepared by Halide Abstraction Using Surface R_3Si^+ Species

*J. Gao, R. W. Dorn, G. P. Laurent, F. A. Perras, A. J. Rossini, M. P. Conley**

General Considerations. All reactions and manipulations were performed under an inert atmosphere of nitrogen or argon using standard glovebox or Schlenk techniques. C_6D_6 was purchased from Cambridge Isotope Laboratories, dried over Na/benzophenone, and freeze-pump-thawed three times before use. Dichloromethane, pentane, and toluene were dried by passing through a double-column J. C. Meyer solvent system and sparged with Ar before use. Pentane and toluene used for vacuum distillation were degassed by three freeze-pump-thaw cycles and stored over Na/benzophenone. Methyl acrylate and cyclohexane were dried over CaH_2 and distilled -before use. All other commercially available reagents were used as received without purification. *N*,*N*′-Bis(2,6-dibenzhydryl-4-methylphenyl)butane-2,3-diimine,[1] *N*,*N*′-Bis(2,6-dibenzhydryl-4-methylphenyl)butane-2,3-diimine palladium methyl chloride,[1] $Al(OC(CF_3)_3)_3(PhF)$[2] and $[^iPr_3Si][(R^FO)_3AlOSi\equiv]$[3] were reported previously. Vinyl chloride and CO were stored over activated sieves and reduced BASF-5 copper catalyst. Polymer grade ethylene 99.97% was passed through a column supplied by Trigon Technologies to remove traces of H_2O/O_2 prior to polymerization reactions. FT-IR spectra were recorded as pressed pellets using a Bruker Alpha IR spectrometer in an argon-filled glovebox. Gas chromatographs were recorded on a Agilent 7820A GC system equipped with an HP-PLOT Q column. Details about temperature programs for GC measurements are provided in the Supporting Information. C, H, N elemental analyses were performed at the University of California, Berkeley. ICP-OES were measured on a Perkin-Elmer Optima 7300DV at the UCR Environmental Sciences Research Laboratory (ESRL). Images of polymers were recorded on a ThermoFisher Scientific NNS450 Scanning Electron Microcope at the Central Facility for Advanced Microscopy and Microanalysis (CFAMM) at UCR.

NMR Spectroscopy. Solution ^1H and ^{13}C NMR spectra were recorded on Avance Bruker 7.05 T (^1H = 300 MHz), or Avance Bruker 14.1 T (^1H = 600 MHz) NMR spectrometers. Chemical shift (δ) were referenced to the NMR chemical shift of residual solvent peaks.

Solid-state NMR spectra were acquired using either a (^1H and ^{13}C spectra) 14.1 T Bruker NEO spectrometer (^1H = 600 MHz), (^1H-^{19}F spectra) a 9.4 T Agilent DD2 spectrometer, or (^{13}C-^{27}Al) a 9.4 T Bruker Avance III spectrometer equipped with a liquid N_2 cooling cabinet. All solid-state NMR samples were packed and sealed in appropriately sized rotors in a glovebox under an inert atmosphere of Ar or N_2. The NMR rotors were sealed with either (^{13}C-^{27}Al, 3.2 mm sapphire rotor) a silicone plug or (^1H-^{19}F, 3.2 mm zirconia rotor) inserts containing 2 protonated/fluorinated O-rings (on both sides of the rotor). Chemical shifts for all solid-state NMR spectroscopy experiments were referenced to the ^1H chemical shifts of neat tetramethylsilane using either adamantane (δ_{iso} = 1.82 ppm) or sodium trimethylsilylpropanesulfonate (d_{iso} = 0.00 ppm) as a secondary reference. ^{13}C, ^{19}F, and ^{27}Al shifts were referenced using previously reported IUPAC relative NMR frequencies.[4]

^1H-^{19}F HETCOR NMR experiments were performed with a 20 kHz MAS frequency and with the NMR probe cooled to –40 °C. $^1H\{^{19}F\}$ D-HMQC and S-REDOR expeirments were performed with $SR4_1^2$heteronuclear dipolar recoupling[5] applied to the ^1H spins. $^{13}C\{^{27}Al\}$ PM-RESPDOR[6] expeirments were performed with 10 kHz MAS, a sample temperature of ~ 100 K, REDOR heteronuclear dipolar recoupling applied to the ^{13}C spins (50 kHz RF field), and $^1H\rightarrow{}^{13}C$ CP (1 ms contact time) at the beginning of the experiment. SPINAL64 heteronuclear decoupling with a 100 kHz ^1H RF field was performed during the entire $^{13}C\{^{27}Al\}$ PM-RESPDOR experiment.[7] A frequency splitter (REDOR box) was used on the X-channel of the NMR probe to split the resonance frequency and simulatanously tune the probe to both ^{13}C and ^{27}Al.

GPC Measurements. High-GPC measurements were performed using an Agilent 1260 Infinity II High Temperature GPC that incorporates a differential refractive index detector. HPLC grade 1,2,4-Trichlorobenzene (TCB) was used as the mobile phase at a flow rate of 1 mL min^{-1}. Columns and detectors were maintained at 140°C. All polymers were injected at a concentration of 0.5 mg mL^{-1} and filtered through a 0.2 µm PTFE filter prior to analysis. Calibration was made by polystyrene standards

and was corrected for linear polyethylene by universal calibration using the Mark-Houwink parameters for polyethylene.

Synthesis of (cod)Pd($^{13}CH_3$)Cl. Iodomethane-^{13}C (2.5 mL, 40 mmol) dissolved in diethyl ether (50 mL) was added dropwise to a mixture of Mg turnings (1.2 g, 50 mmol) suspended in diethyl ether (50 mL) under Ar at room temperature. The mixture was stirred at room temperature for 2h, which resulted in the dissolution of most of the Mg turnings. The mixture was cooled to 0 °C with an ice bath and a solution of $SnCl_4$ in pentane (1M solution, 8 mL, 8 mmol) was added dropwise to the $^{13}CH_3MgI$ solution and stirred overnight at room temperature. The reaction was quenched by adding water (5 mL) at 0°C and dried with Na_2SO_4. After filtration to remove Na_2SO_4, the solvents were removed by distillation at atmospheric pressure to give crude $Sn(^{13}CH_3)_4$ (0.88 g, 4.81 mmol, 60 % yield), which was used in the next step without further purification. (cod)$PdCl_2$ (0.57 g, 2 mmol) was dissolved in 30 mL DCM and $Sn(^{13}CH_3)_4$ (0.88 g, 4.81 mmol) was added at room temperature under Ar. The mixture was stirred at room temperature for 24h. The solution was filtered through celite, and the filtrate was evaporated to dryness under vacuum. The solid residue was washed with diethyl ether (3*3 mL) to afford an off-white solid (320 mg, 60%). ^{1}H NMR (300 MHz, C_6D_6): 5.65 (m, 2H). 4.19 (m, 2H), 1.44-1.59 (m, 8H), 1.34 (d, 3H, $^1J_{CH}$ = 140.1 Hz, Pd-$^{13}CH_3$). ^{13}C NMR (75.4 MHz, C_6D_6): 123.55, 100.19, 30.68, 27.37, 11.79 (Pd-$^{13}CH_3$). Anal. Calcd for $C_8{}^{13}CH_{15}PdCl$: C, 41.00; H, 5.68. Found: C, 40.66; H, 5.38.

Preparation (N^N)Pd($^{13}CH_3$)Cl. (cod)Pd($^{13}CH_3$)Cl (0.26 g, 1 mmol) and *N*,*N*′-Bis(2,6-dibenzhydryl-4-methylphenyl)butane-2,3-diimine (0.93 g, 1 mmol) were dissolved in CH_2Cl_2 (20 mL) and stirred at room temperature for 2 days. After this time the solvent was removed under vacuum the solid was purified by column chromatography using CH_2Cl_2 as eluent to afford the desired product as a red solid (360 mg, 33%). ^{1}H NMR (300 MHz, $CDCl_3$): 7.51 (d, J = 7.2 Hz, 4H, aryl-H), 7.41 (d, J = 6.3 Hz, 4H, aryl-H), 7.32 - 7.06 (m, 34H, aryl-H) 6.81 (s, 2H, aryl-H), 6.04(s, 2H, C*H*Ph2), 5.77 (s, 2H, C*H*Ph2), 2.30 (s, 3H, C*H*$_3$), 2.22 (s, 3H, C*H*$_3$), 0.67 (d, 3H, $^1J_{CH}$ = 136.0 Hz, Pd-^{13}C*H*$_3$), 0.44 (s, 3H, N=C*Me*), 0.19 (s, 3H, N=C*Me*). ^{13}C NMR (75.4 MHz, $CDCl_3$): δ 177.53 (N=*C*Me), 172.97(N=*C*Me), 143.93, 142.46, 142.31, 142.30, 140.94, 136.24, 135.23, 134.62, 133.97, 130.13, 129.93, 129.88, 129.64, 128.67, 128.62, 128.52, 128.17, 126.91, 126.63, 126.49, 126.33, 51.69 (C*H*Ph$_2$), 51.35 (C*H*Ph$_2$), 21.60 (*C*H$_3$), 21.54 (*C*H$_3$), 20.36 (N=C-*Me*), 19.34 (N=C-*Me*), 5.86 (Pd-^{13}*C*H$_3$). Anal. Calcd for $C_{71}{}^{13}CH_{65}PdN_2Cl_3$(+1.5 CH_2Cl_2): C, 71.57; H, 5.25; N, 2.35. Found: C, 71.40; H, 6.09; N 2.16.

*Preparation of **1**.* [^{i}Pr$_3$Si][(R^{F}O)$_3$AlOSi≡] (500 mg, 0.2 mmol R_3Si^+ g^{-1}) and (N^N)Pd(CH_3)Cl (0.14 g, 0.26 mmol) were transferred to one arm of a double-Schlenk flask inside an argon-filled glovebox. Toluene (~ 15 mL) was transferred under vacuum to the arm of the flask containing [^{i}Pr$_3$Si][(R^{F}O)$_3$AlOSi≡] and (N^N)Pd(CH_3)Cl at 77 K. The red slurry was stirred at room temperature for 30 minutes. The clear red solution was filtered to the other side of the double Schlenk. The remaining solid was washed by condensing solvent from the other arm of the double Schlenk at 77 K, warming to room temperature, stirring for 5 minutes, and filtering the solvent back to the other side of the flask. This procedure was repeated several times until the color of toluene was colorless when stirred with the supported Pd catalyst. (N^N)Pd(CH_3)Cl is only modestly soluble in toluene, and five washes were necessary to remove all (N^N)Pd(CH_3)Cl. The orange solid was dried under diffusion pump vacuum for an hour and stored in a glovebox freezer at -20 °C. An identical procedure was used to prepare **1-^{13}C**. Elemental analysis for **1**; C: 8.33 %; H: 0.42 %; N: 0.08 %. Pd content was determined by ICP-OES after digestion as described in the Supporting Information. Three independent measurements give 0.048 ± 0.001 mmol Pd/g. A procedure describing the determination of ^{i}Pr$_3$SiCl evolved during this reaction is given in the Supporting Information.

*Reaction of 1 with Vinyl Chloride***.** A Teflon valved 100 mL flask was charged with **1-^{13}C** (100 mg) in an Ar-filled glovebox. The flask was connected to a vacuum line, evacuated, and vinyl chloride (0.55 mmol, 100 equiv.) was transferred into the flask at 77K. The Teflon valve was sealed, and the mixture was heated to 60 ℃ for 3 h. Analysis of the volatiles by gas chromatography (Figure S10) showed that 0.050 ± 0.003 mmol g^{-1} of propene forms in this reaction (average of three independent runs). Solution ^{1}H NMR analysis of the volatiles shows that the ^{13}C label was incorporated in C_3 of propylene (Figure

4a), a full ^{1}H and ^{13}C NMR spectrum of the volatiles in this reaction are shown in Figure S12. Solid-state ^{13}C CPMAS NMR spectra of **1** and **2** are shown in Figure S11.

General Procedure for Polymerization Reactions. Polymerization reactions were performed in a Biotage Endeavor 8 well parallel high-pressure reactor in an N_2 filled glovebox. The 15 mL glass reaction sleaves were charged with **1** (9 mg, 0.5 μmol Pd) and 5 mL of cyclohexane or toluene. The Biotage was sealed and pressurized with 150 psi (10.3 bar) ethylene on demand and heated to the desired temperature. After 30 minutes, the Biotage was vented, the glass reaction sleaves were removed from the glovebox, and treated with 5% aqueous HCl in methanol (15 mL) to precipitate polymers. The polymers were isolated by filtration and dried under vacuum to constant weight (~ 2h). Copolymerization reactions with methyl acrylate used a similar procedure, except a solution of methyl acrylate (1 M) in the desired solvent was added to the reaction, and the Biotage was pressurized with 80 psi ethylene for 15h. The data from the polymerization reactions are given in Table 1 of the main text. A plot showing the activity in ethylene polymerization reactions as a function of temperature and solvent is shown in Figure 5. Solution NMR characterization and GPC traces of the polymers are given in the Supporting Information.

Solution NMR spectra of Compounds:

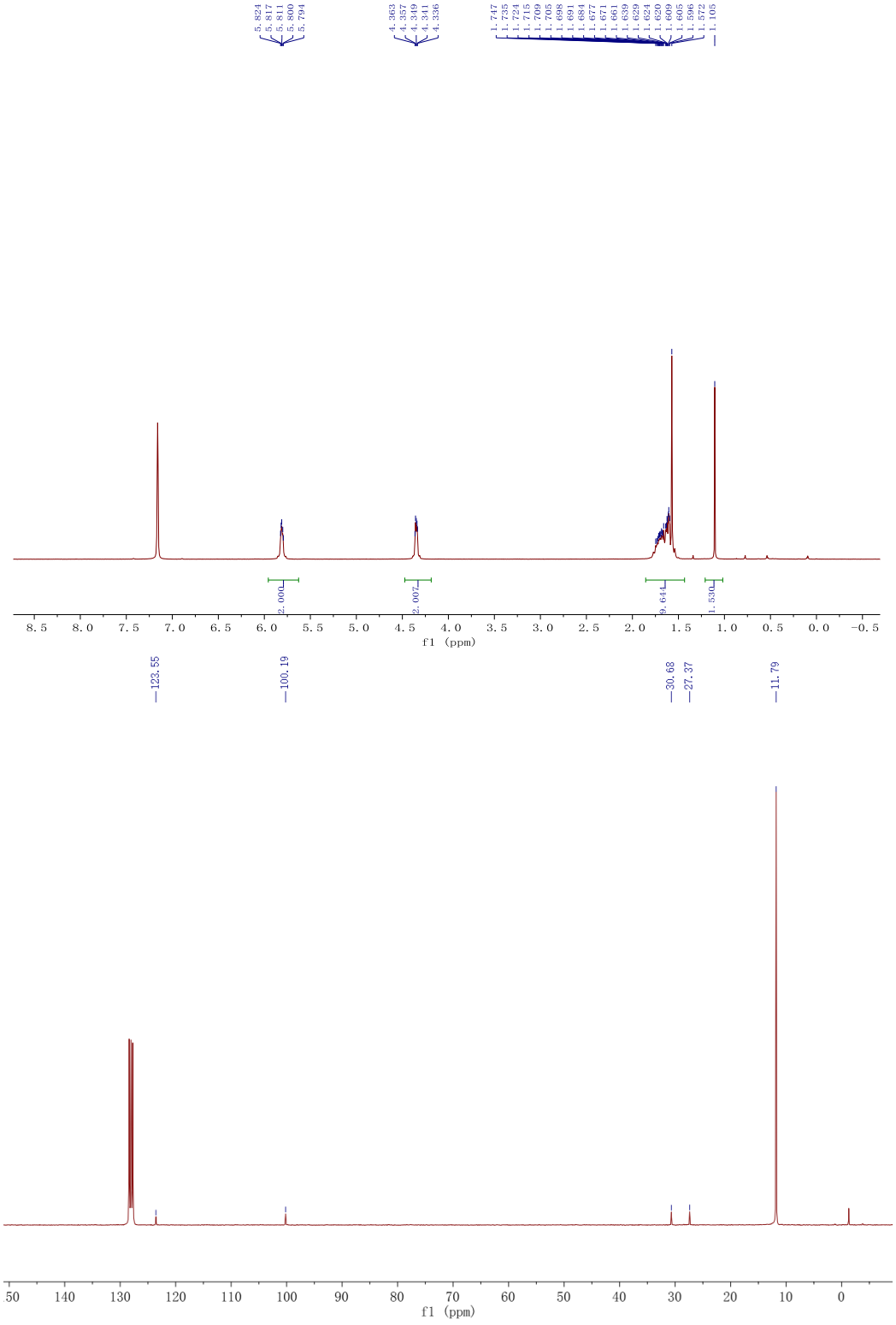

Figure S1. ^{1}H and $^{13}C\{^{1}H\}$ NMR spectra of the (cod)Pd($^{13}CH_3$)Cl

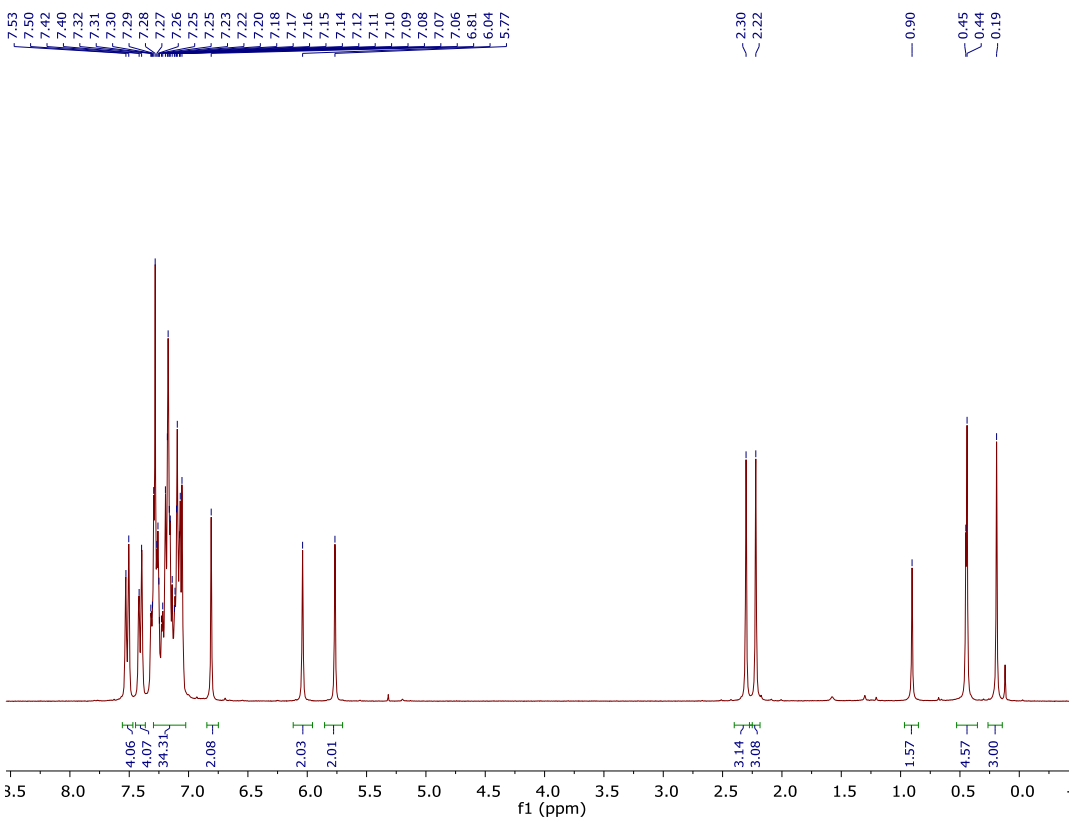

^{1}H NMR Chemical Shift (ppm)

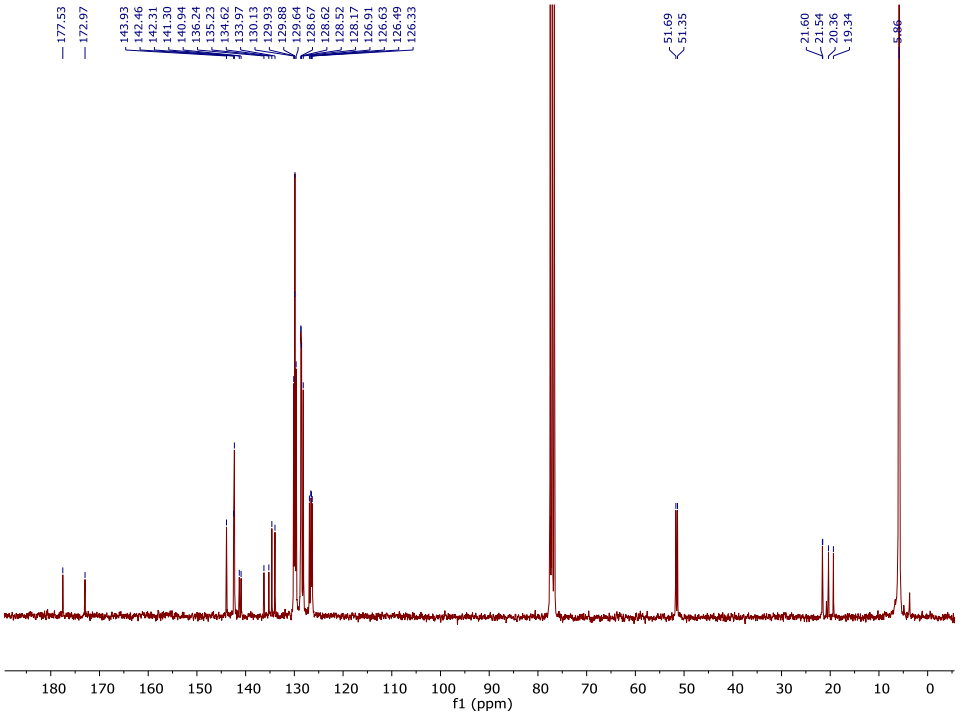

^{13}C NMR Chemical Shift (ppm)

Figure S2. ^{1}H and ^{13}C{^{1}H} NMR spectra of the (N^N)Pd(^{13}CH$_3$)Cl

Solid state NMR spectra of 1 and 1-^{13}C:

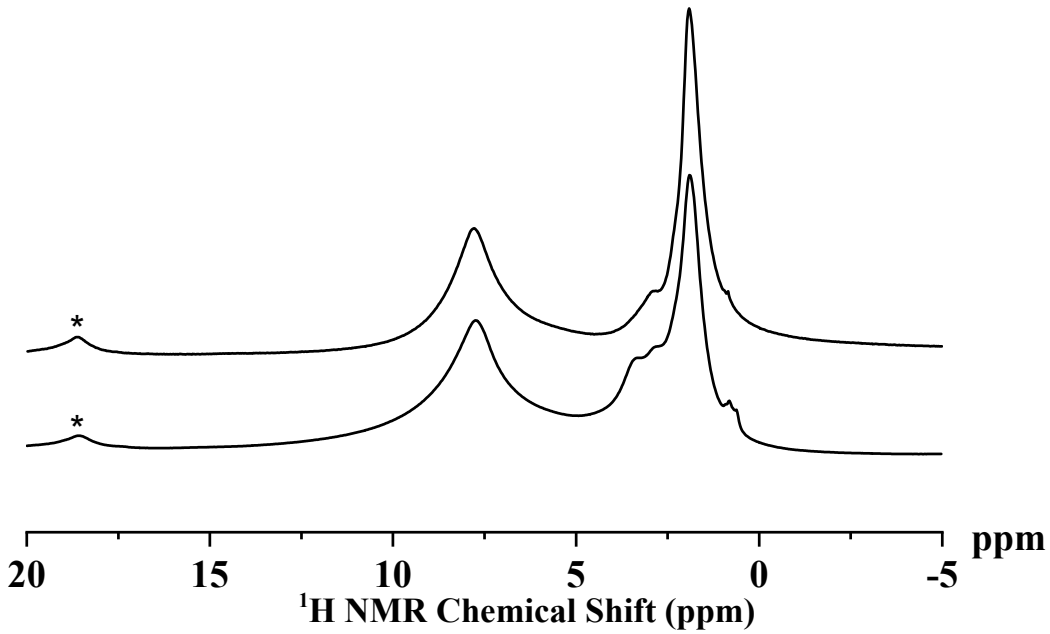

Figure S3.^{1}H NMR spectra of **1** (top) and **1-^{13}C** (bottom). *=spinning sideband

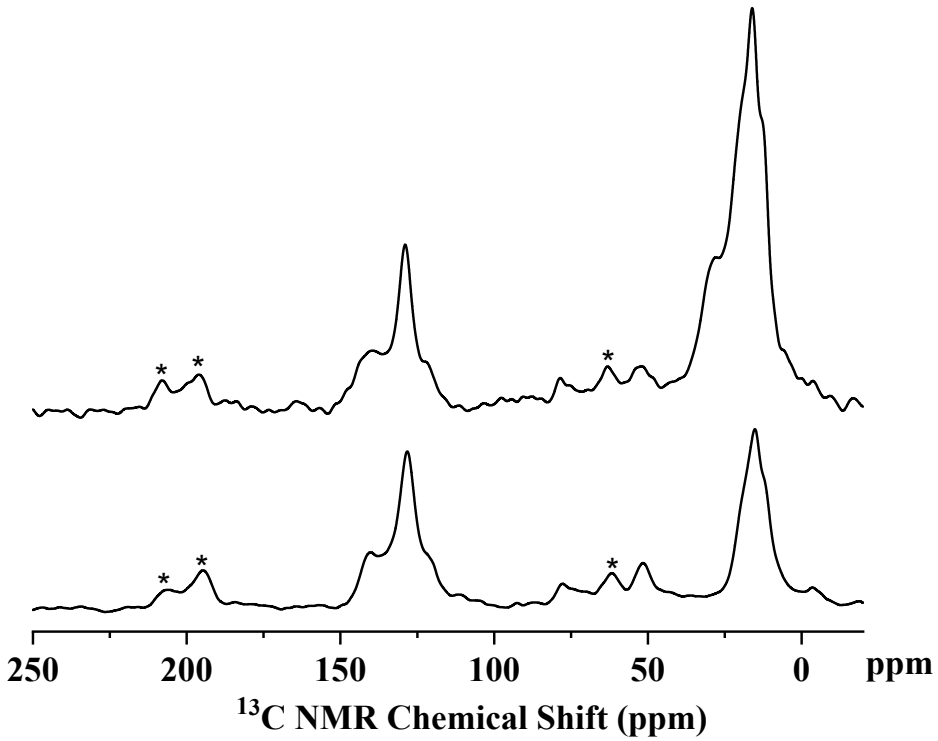

Figure S4. ^{13}C NMR spectra of **1** (bottom) and **1-^{13}C** (top). *=spinning sidebands.

The ^{29}Si CPMAS and static ^{27}Al{^{1}H} NMR spectra of **1** are shown in Figure S5.
^{29}Si{^{1}H} CPMAS NMR (119 MHz, 8 kHz): 70 (≡Si–O*Si*^{i}Pr$_3$--- Al(OR^{F})$_3$), 11 (≡Si– O*Si*^{i}Pr$_3$), 105 (*Si*O$_2$) ppm.
The presence of the peak at 70 ppm in this spectrum is consistent with the solution data above showing that not all R_3Si^+ sites present in [^{i}Pr$_3$Si][(R^{F}O)$_3$AlOSi≡] are reactive towards (N^N)Pd(CH$_3$)Cl.

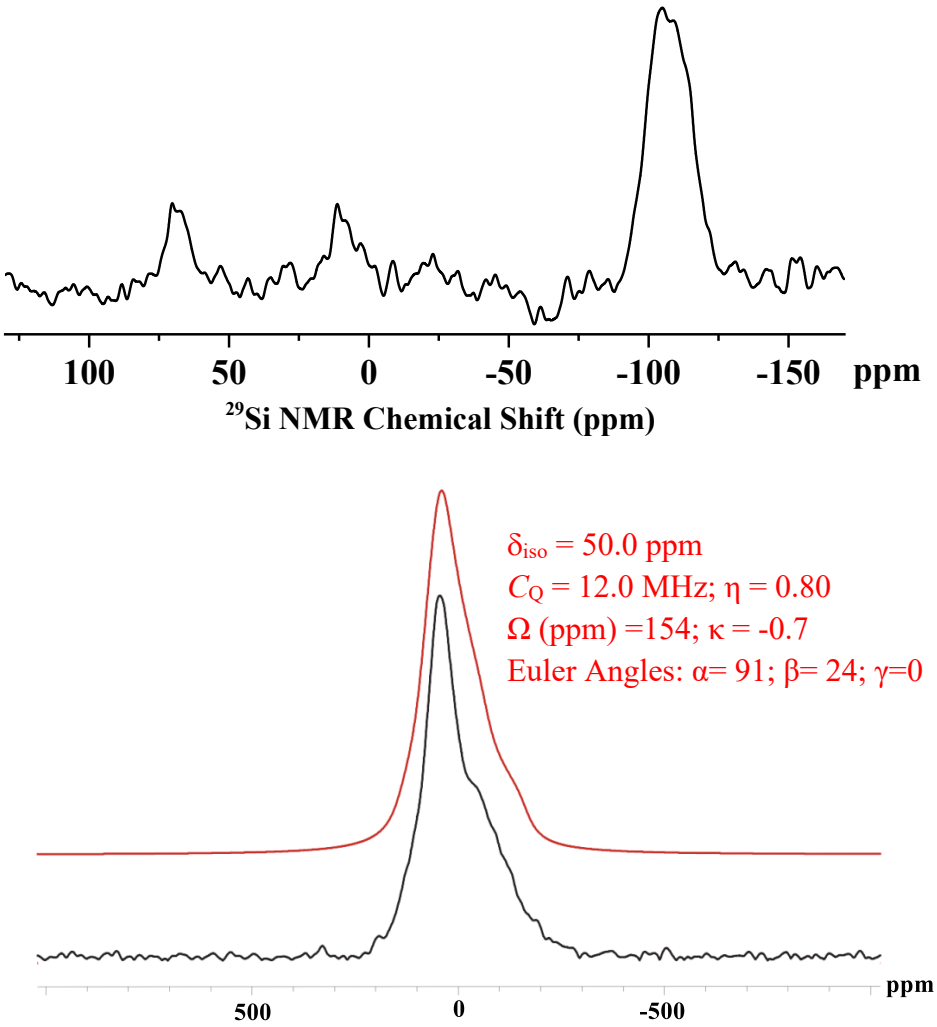

Figure S5. (Upper) ^{29}Si NMR spectrum of **1** and (lower) static ^{27}Al solid state NMR spectrum of **1** (black) and simulation (red).

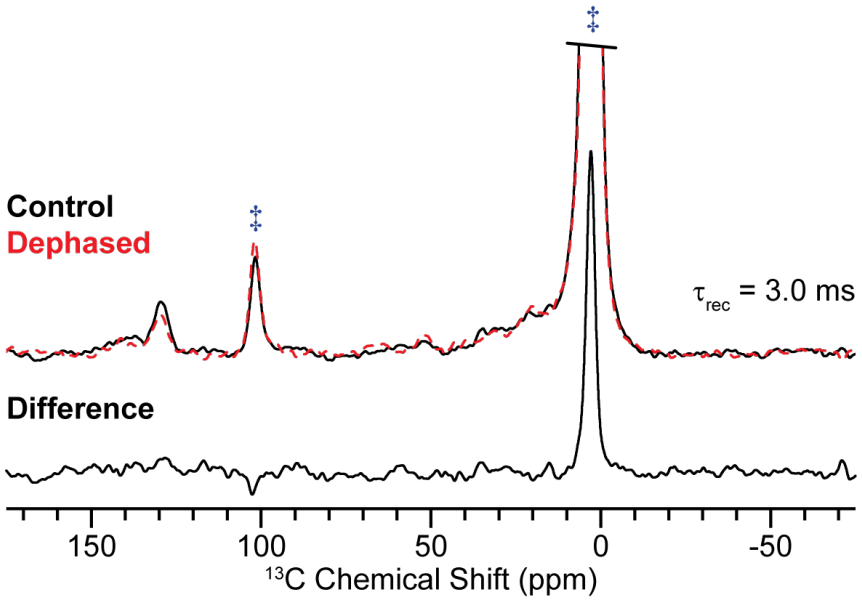

Figure S6. $^{13}C\{^{27}Al\}$ PM-RESPDOR NMR spectra of **1**. The black and red ^{13}C NMR spectra were recorded without or with a phase-modulated (PM) saturation pulse applied to the ^{27}Al spins.[6b] A difference spectrum (control minus dephase) is shown below. NMR spectra were recorded at B_0 = 9.4 T with 3 ms of total REDOR heteronuclear dipolar recoupling (50 kHz RF field) applied to the ^{13}C spins, 10 kHz MAS and a sample temperature of ~ 100 K. $^{1}H \rightarrow {}^{13}C$ CP (1 ms CP contact time) was performed at the beginning of the experiment. A frequency splitter (REDOR box) was applied to the X-channel of the NMR probe to splitting the tuning frequency to both ^{13}C and ^{27}Al. The intense ^{13}C NMR signal at 2 ppm (100 ppm is the spinning sideband) comes from the silicone cap that was used to seal the rotor.

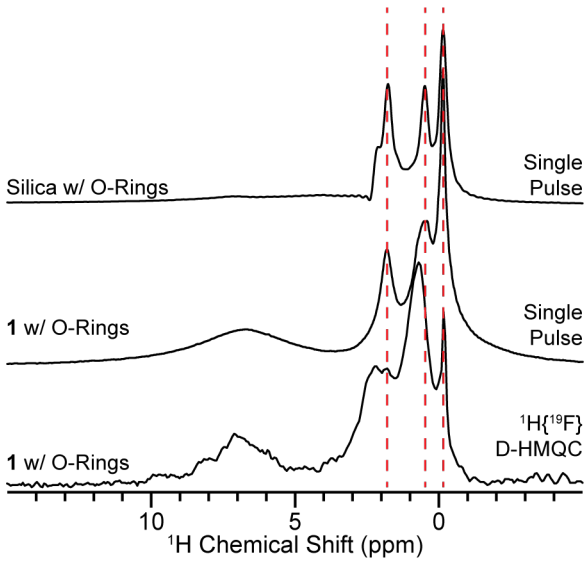

Figure S7. ^{1}H single pulse spectra of (upper) silica and (middle) **1**. All rotors were sealed with protonated/fluorinated O-rings on both sides of the sample. Comparison of the upper and middle spectrum confirms that the ^{1}H NMR signals at *ca.* 7 ppm can be attributed to the phenyl H atoms of **1**. (Lower) 1D ^{1}H{^{19}F} D-HMQC spectrum of **1**.

Discussion of fitting of $^1H\{^{19}F\}$ S-REDOR dephasing curves. Generally, REDOR dephasing curves in multispin systems, particularly in the initial rise, are well-represented by the result of a two-spin simulation if the dipolar coupling constant, D_{HF}, is replaced by the root sum squares of the different spin pairs: $\sqrt{\sum D_{HF}^2}$.[8] As described below, the relationship between the ^1H-^{19}F dipolar coupling constants and the S-REDOR dephasing observed in multispin systems allowed us to determine the average Pd-Al internuclear distance between the (N^N)Pd-CH_3^+ group and the [$(R^FO)_3$Al-OSi≡] surface anion.

We constructed a model consisting of a single (N^N)Pd-CH_3^+ molecule and a single [$(R^FO)_3$Al-OSi≡] surface anion, with a variable Al-Pd distance (Figure 3c of the main text). For this purpose, the single-crystal X-ray structure of (N^N)Ni-Br_2 was used to obtain a reasonable structural model of (N^N)Pd-CH_3^+; the two Br atoms were removed from the structure, and the Ni atom was replaced with Pd.[1a] A [$((CF_3)CO)_3AlO^-$] molecule was then constructed in the open-source Avogadro[9] program with an assumed tetrahedral geometry at the Al center and was arranged such that one of the fluoro *t*-butoxide ligands was directed towards the (N^N)Pd-CH_3^+ molecule, in the pocket formed by the (N^N) ligand (Figure 3c of the main text). The [$((CF_3)CO)_3AlO^-$] and (N^N)Pd-CH_3^+ molecules were also arranged such that the Pd and Al atoms were in the same plane; this was achieved by exporting the XYZ coordinates of both moleulces into a spreadsheet and adjusting the X, Y and Z coordinate of both molecules, such that the Al and Pd atom had the same Z component (the spreadsheet was uploaded as a separate supporting information file). Therefore, the Pd-Al internuclear distance could be adjusted by simultaneously changing the X and Y coordinate of one molecule by the Pd-Al distance divided by $\sqrt{2}$ (we chose to move the [$((CF_3)CO)_3AlO^-$] molecule).

For a given Pd-Al distance, the internuclear distance between each phenyl H atom of (N^N)Pd-CH_3^+ and all F atoms of the [$(R^FO)_3$Al-OSi≡] surface anion were calculated, enabling the determination of $\sqrt{\sum D_{HF}^2}$ for each H site. We then converted the determined $\sqrt{\sum D_{HF}^2}$ for each H site back to an effective ^1H-^{19}F two-spin dipolar coupling and internuclear distance. At this point, for a given Pd-Al internuclear distance, we have calculated the effective ^1H-^{19}F internuclear distance for each phenyl H atom of (N^N)Pd-CH_3^+. Therefore, we could determine the *mean* effective ^1H-^{19}F internuclear distance by taking the average of all effective ^1H-^{19}F internuclear distances, as well as the *standard deviation* of the effective ^1H-^{19}F internuclear distances for a given Pd-Al internuclear distance (Figure S8 and Table S1).

The experimental $^1H\{^{19}F\}$ S-REDOR curve was then fitted to numerically simulated $^1H\{^{19}F\}$ S-REDOR curves. 51 numerical two-spin simulations were performed with ^1H-^{19}F dipolar coupling constants corresponding to internuclear distances ranging from 1.0 Å to 11.0 Å in steps of 0.2 Å. A Gaussian distribution of all 51 numerically simulated curves was used with the proper statistical weighting factors to resemble the *standard deviation* in the effective ^1H-^{19}F internuclear distance for a given Pd-Al distance. For example, if the Pd-Al internuclear distance was 11 Å, $\sqrt{\sum D_{HF}^2}$ was calculated and then converted back to an effective ^1H-^{19}F internuclear distance for each phenyl H atom. We then averaged over all phenyl H atoms effective ^1H-^{19}F internuclear distances to determine the *mean* effective ^1H-^{19}F internuclear distance and its *standard deviation*. We then fitted the experimental $^1H\{^{19}F\}$ S-REDOR curve to a Gaussian distribution of numerically simulated $^1H\{^{19}F\}$ S-REDOR curves with the same *mean* effective ^1H-^{19}F internuclear distance and its *standard deviation* determined above. We then repeated this process for different Pd-Al internuclear distances until we reached a satisfactory fit to the

experimental curve. Using this procedure, the best fit Pd-Al internuclear distance was determined to be 11 Å (Figure 3b of the main text). A Pd-Al distance of 11 Å places the [$(R^FO)_3$Al-OSi≡] surface anion at a chemically reasonable distance from the (N^N)Pd-CH_3^+ fragment (Figure 3c of the main text), with the closest ^{1}H-^{19}F distance being 1.8 Å.

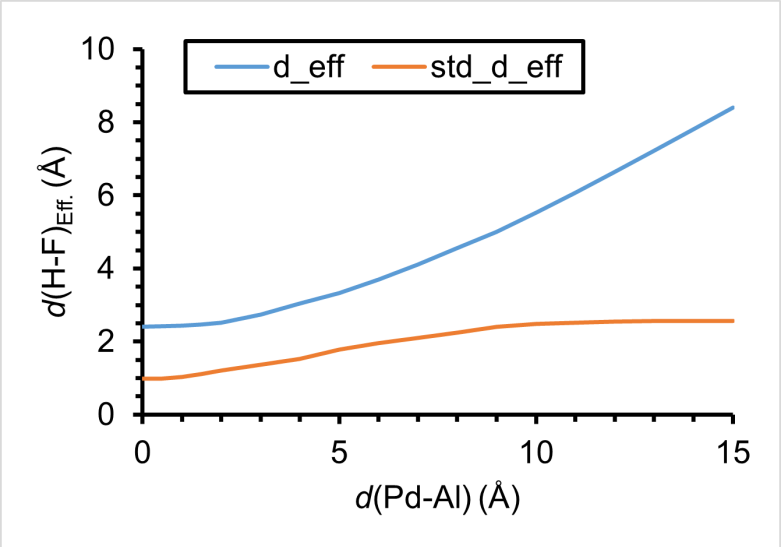

Figure S8. (blue) The mean effective two-spin ^{1}H-^{19}F internuclear distance and (orange) standard deviation of two-spin ^{1}H-^{19}F internuclear distances for the ^{1}H{^{19}F} S-REDOR model of **1**.

Table S1. The mean effective two-spin ^{1}H-^{19}F internuclear distance and the corresponding standard deviation for the $^{1}H\{^{19}F\}$ S-REDOR model of **1**.

d(Al-Pd) (Å)	$d(H\text{-}F)_{Eff.}$ (Å)	STD of $d(H\text{-}F)_{Eff.}$ (Å)
0	2.405	0.986
0.5	2.424	0.985
1	2.439	1.035
1.5	2.464	1.116
2	2.520	1.207
3	2.744	1.363
4	3.044	1.533
5	3.327	1.78
6	3.694	1.963
7	4.114	2.103
8	4.554	2.247
9	5.010	2.400
10	5.526	2.477
11	6.075	2.519
12	6.643	2.543
13	7.224	2.555
14	7.813	2.561
15	8.405	2.563

Determination of $^{i}Pr_3Si–Cl$ formed during the reaction

To determine the amount of $^{i}Pr_3Si–Cl$ evolved during this reaction, [$^{i}Pr_3Si$][$(R^FO)_3AlOSi\equiv$] (10 mg, 0.002 mmol R_3Si^+), (N^N)Pd(CH_3)Cl (3.3 mg, 0.003 mmol), and hexamethylbenzene (HMB) (5 mg, 0.03 mmol) were loaded into a Teflon valved NMR tube. C_6D_6 (0.5 mL) was added to the NMR tube, and the reaction was monitored by using ^{1}H NMR spectroscopy. After 30 minutes reaction time integration of the $^{i}Pr_3Si$-Cl signal with respect to the hexamethylbenzene internal standard showed that 0.055 mmol $^{i}Pr_3Si–Cl$ evolved (0.055 mmol g^{-1} SiO_2), and that longer reaction times do not result in significant increases in $^{i}Pr_3Si–Cl$ concentration (Figure S9). Identical $^{i}Pr_3Si–Cl$ concentrations were observed using (N^N)Pd($^{13}CH_3$)Cl. Table S2 gives data for five independent halide abstraction reactions, showing the reproducibility of this procedure.

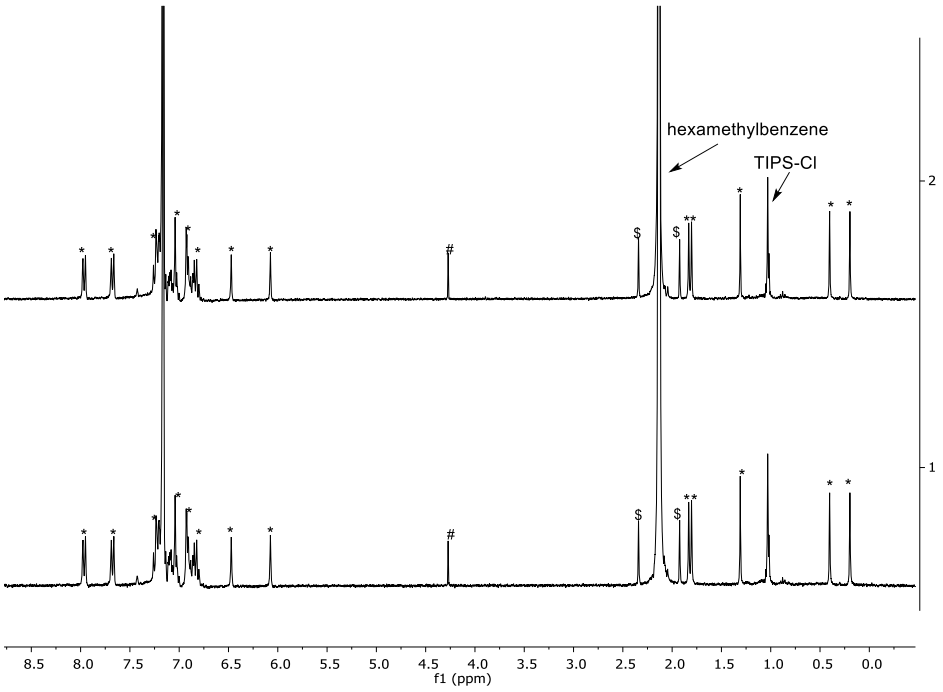

Figure S9. ^{1}H NMR reaction between (N^N)Pd($^{13}CH_3$)Cl with [$^{i}Pr_3Si$][$(R^FO)_3AlOSi\equiv$] after 30 minute (bottom spectrum) and 1h (top spectrum). *= N^N Pd(CH_3)Cl, #=DCM, $=satellite peak of hexamethylbenzene.

Table S2. Quantification of $^{i}Pr_3Si–Cl$ generated in the reaction.

Entry	Integral of C_6Me_6	Integral of $^{i}Pr_3Si–Cl$	$^{i}Pr_3SiC$ yield (mmol/g)
1	18	0.92	0.054
2	18	0.94	0.055
3	18	0.93	0.054
4	18	0.91	0.053
5	18	0.95	0.056

Digestion of 1 for ICP-OES analysis

The Pd digesting method was reported previously with slightly modification[10]: **1** was put into a 60 mL fisher porter with a magnetic stirrer bar. 15 mL hydrochloric (37%) and 5 mL hydrogen peroxide (30%) was added slowly under stirring. The fisher porter was sealed and heated at 90 ℃ overnight.

Table S3. Quantification of Pd loading from ICP-OES analysis.

Entry	Amount of **1** (mg)	Solvent volume (mL)	Pd (ppm)	Pd loading (mmol/g)
1	15	20	3.954	0.0495
2	20	20	5.001	0.0470
3	20	20	4.956	0.0465

The obtained Pd loading was based on this equation (ppm = mg/L):

$$\text{Pd loading (mmol/g)} = \frac{\left\{\left(\frac{mg(Pd)}{L}\right) * \frac{1 mmol\ Pd}{106.42\ mg\ Pd} * Volume\ of\ Solvent\ (L)\right\}}{amount\ of\ \mathbf{1}(mg)}$$

GC parameters

The GC column oven was held at 150 °C for 5 min and the temperature was subsequently raised to 200 °C at 20°C min^{-1} for another 2 min. 200 µL of gas was injected using a split ratio of 76.926:1. He was used as the carrier gas at a flow rate of 23.5 mL/min. The temperature of the flame ionization detector (FID) was set at 350 °C at a flow rate of air and hydrogen at 400 mL/min and 30 mL/min, respectively. In order to quantify the amount of gas, the response factor of the FID was calibrated to known pressures of methane. FID response for hydrocarbons is proportional to the number of carbon atoms in the analyte. The amount of propene was calculated based on this equation:

$$\frac{\left(\frac{Area\ of\ peak}{Number\ of\ carbon\ atoms}\right)}{Responce\ factor} \times V(L) = n(mol)RT(K)$$

Characterization of reaction between vinyl chloride with 1-^{13}C

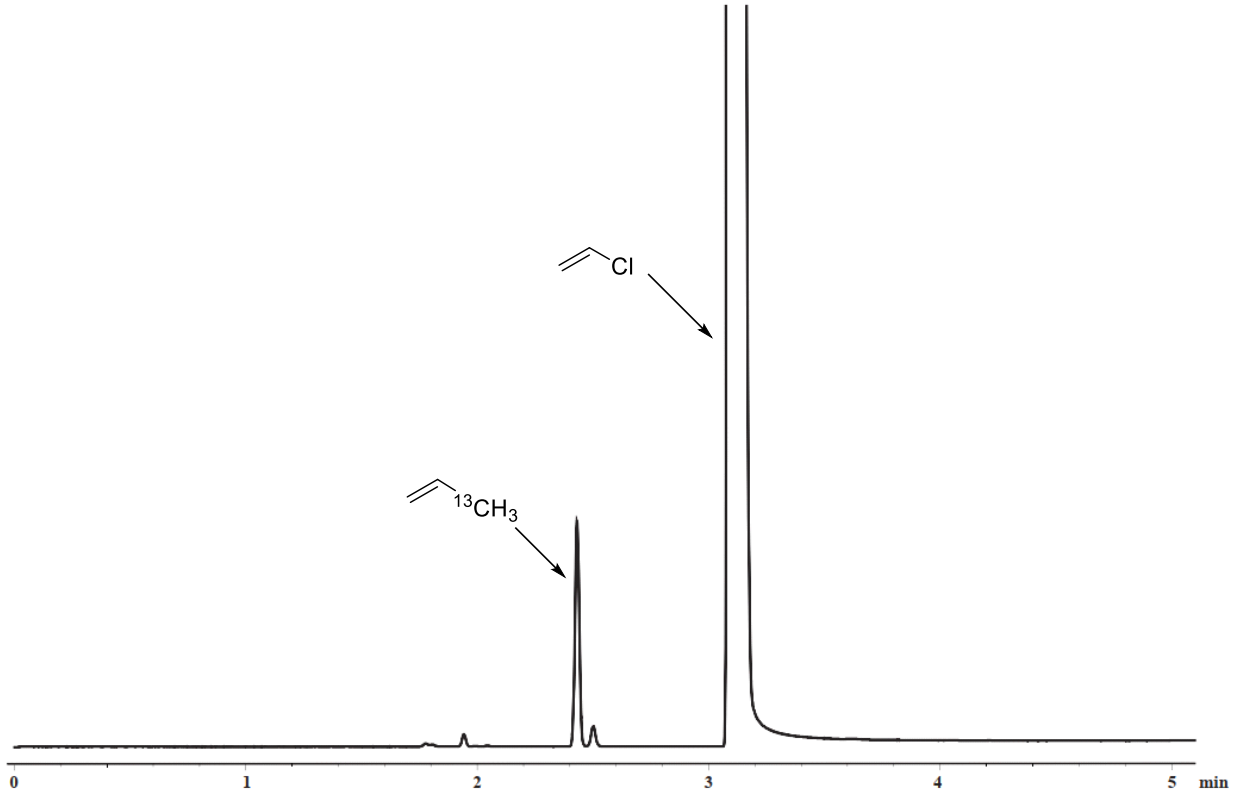

Figure S10. GC of volatiles in reaction of **1-^{13}C** with vinyl chloride. The peak at around 2 minutes is the background peak from the injection. The peak near ^{13}C-propene is an impurity from vinyl chloride.

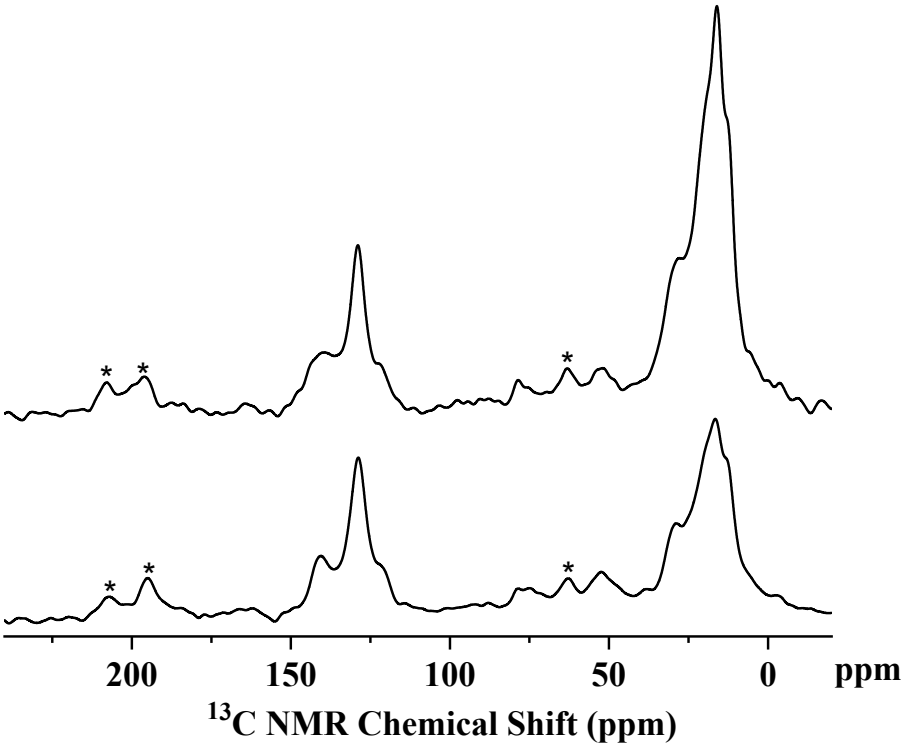

Figure S11. ^{13}C NMR spectra of **1-^{13}C** (top) and **1-^{13}C** after reaction with vinyl chloride (bottom). *=spinning sidebands.

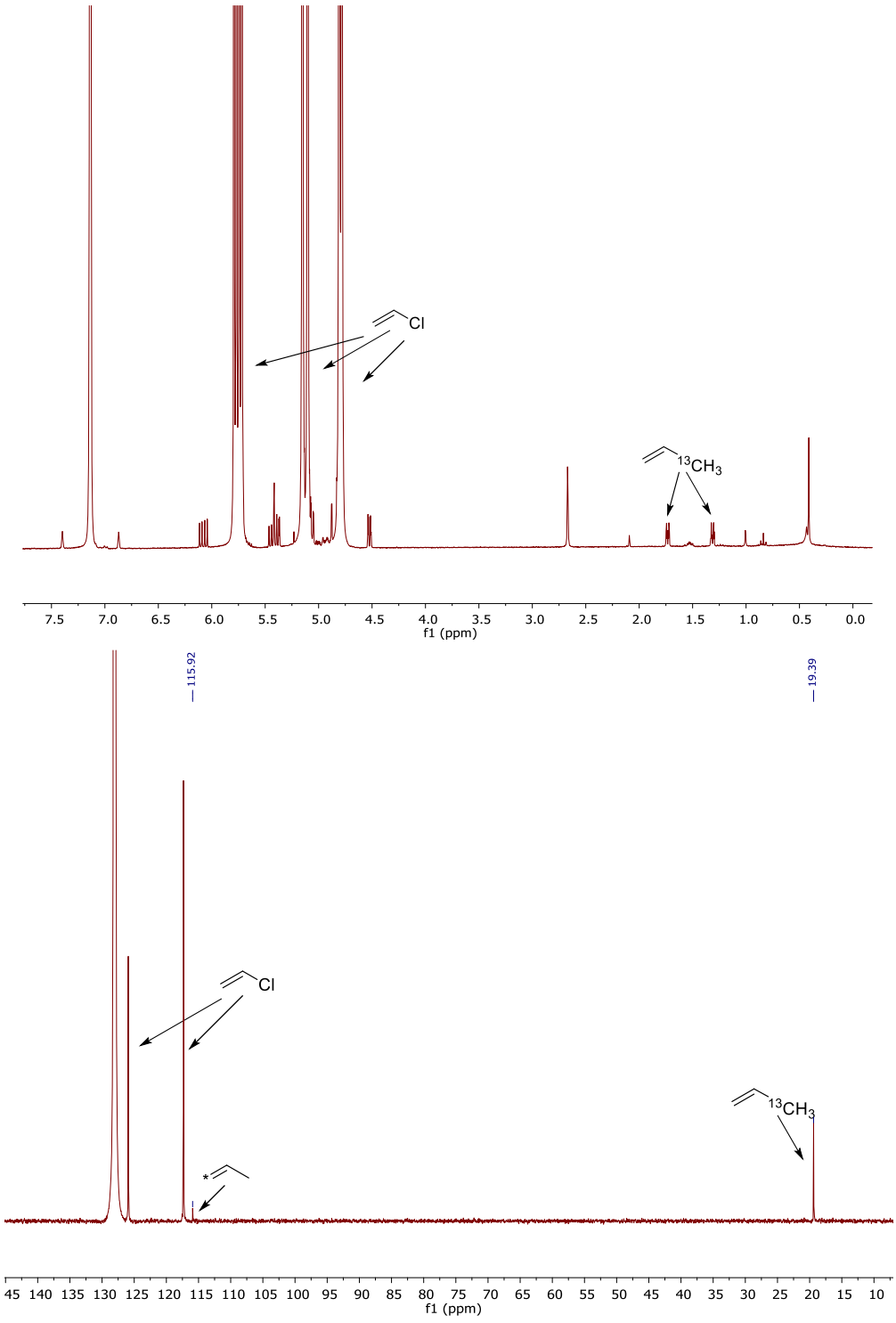

Figure S12. ^{1}H and $^{13}C\{^{1}H\}$ NMR of volatiles in the reaction of **1-^{13}C** with vinyl chloride.

Isomerization of 3-^{13}C-Propene to 1-^{13}C-Propene

The reaction of 100 mg **1-^{13}C** and 200 equiv of vinyl chloride was performed as described in the experimental section. After the reaction was complete, the gas phase (~4:1 3-^{13}C-propene:1-^{13}C-propene and residual vinyl chloride) was vacuum transferred at 77 K to a 50 mL flask containing 100 mg [^{i}Pr$_3$Si][(R^{F}O)$_3$AlOSi≡]. The flask was sealed and heated at 60 ℃ overnight. After this period the volatiles were vacuum transferred to an NMR tube at 77 K containing C_6D_6 and analyzed by ^{1}H NMR spectroscopy. The methyl region of this spectrum is shown in Figure S13 and shows that most of the 3-^{13}C-propene was converted to 1-^{13}C-propene.

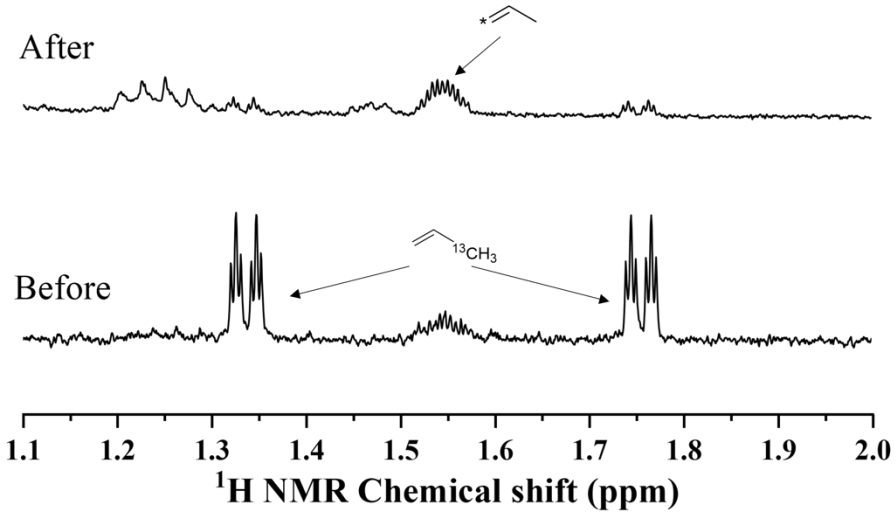

Figure S13. ^{1}H NMR spectrum from 1.1 – 2.0 ppm of volatiles from the reaction of **1-^{13}C** with vinyl chloride produces mostly 3-^{13}C-propene (bottom spectrum). After heating 3-^{13}C-propene with [^{i}Pr$_3$Si][(R^{F}O)$_3$AlOSi≡] mostly 1-^{13}C-propene is present in this NMR spectrum.

Characterization of homopolymer and copolymer

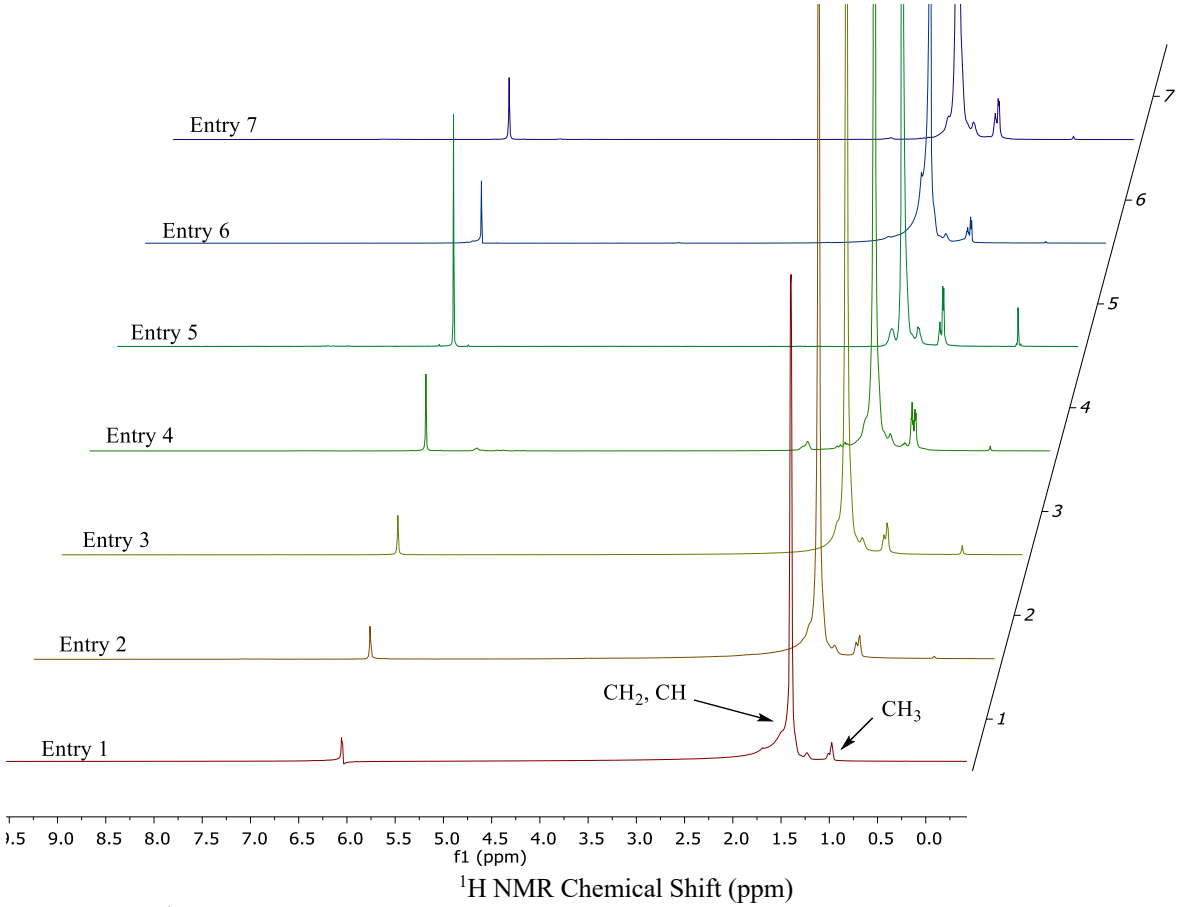

Figure S14. ^{1}H NMR spectra of PE catalyzed over **1**. The NMR spectra were recorded in $C_2D_2Cl_4$ and contained ~ 10 mg of polymer at 120 °C. The stacked NMR spectra correspond to the entries from Table 1 given in the main text.

Polymer branching density was analyzed by ^{1}H NMR spectroscopy:

$$BD = 1000 \times \frac{2 \times I(CH_3)}{3 \times I(CH_2 + CH + CH_3)}$$

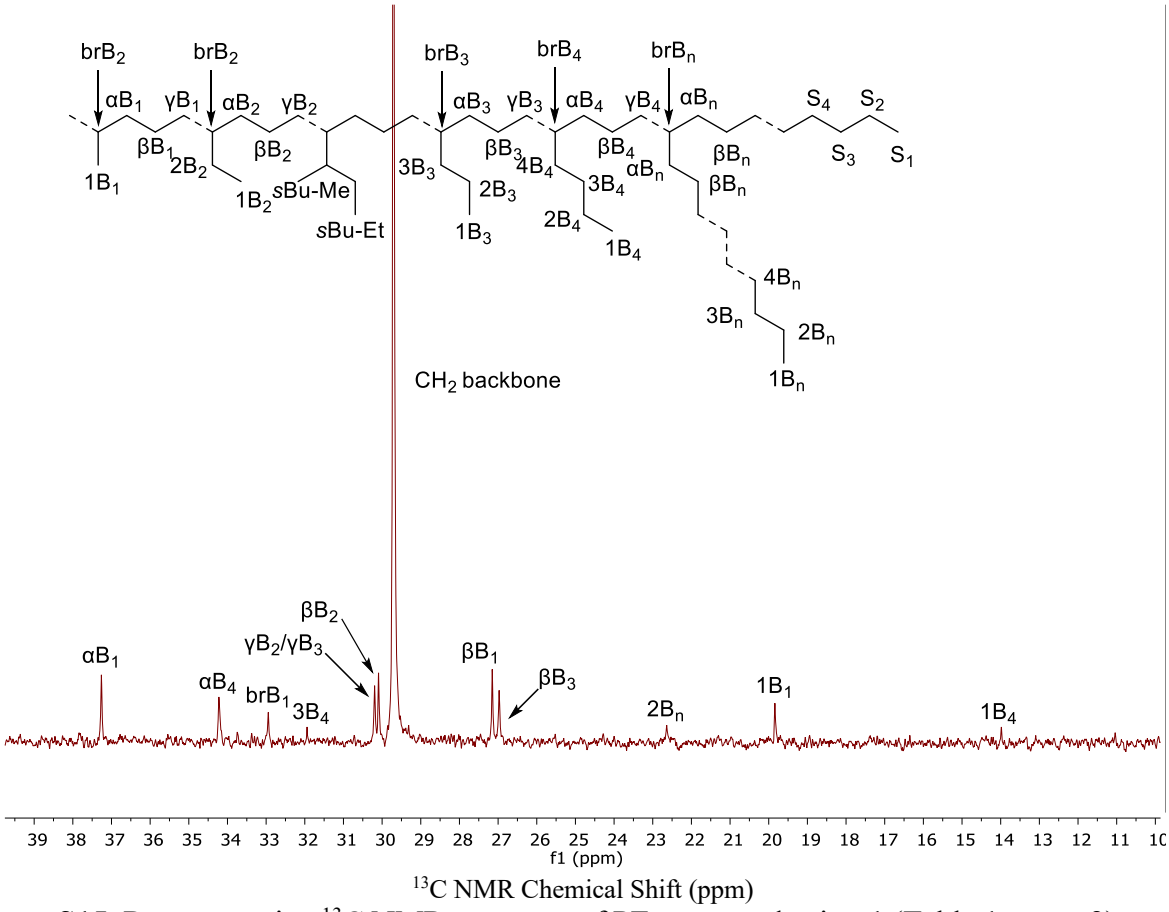

^{13}C NMR Chemical Shift (ppm)

Figure S15. Representative ^{13}C NMR spectrum of PE generated using **1** (Table 1, entry 2) recorded in $C_2D_2Cl_4$ at 120 °C.

The incoporation ratio of MA was calculated from [11]:

$$\text{Incorporation ratio (\%)}=\frac{\frac{I(OMe)}{3}}{\frac{I(OMe)}{3}+\frac{I(CH_2,CH)+I(CH_3)-2}{4}}*100$$

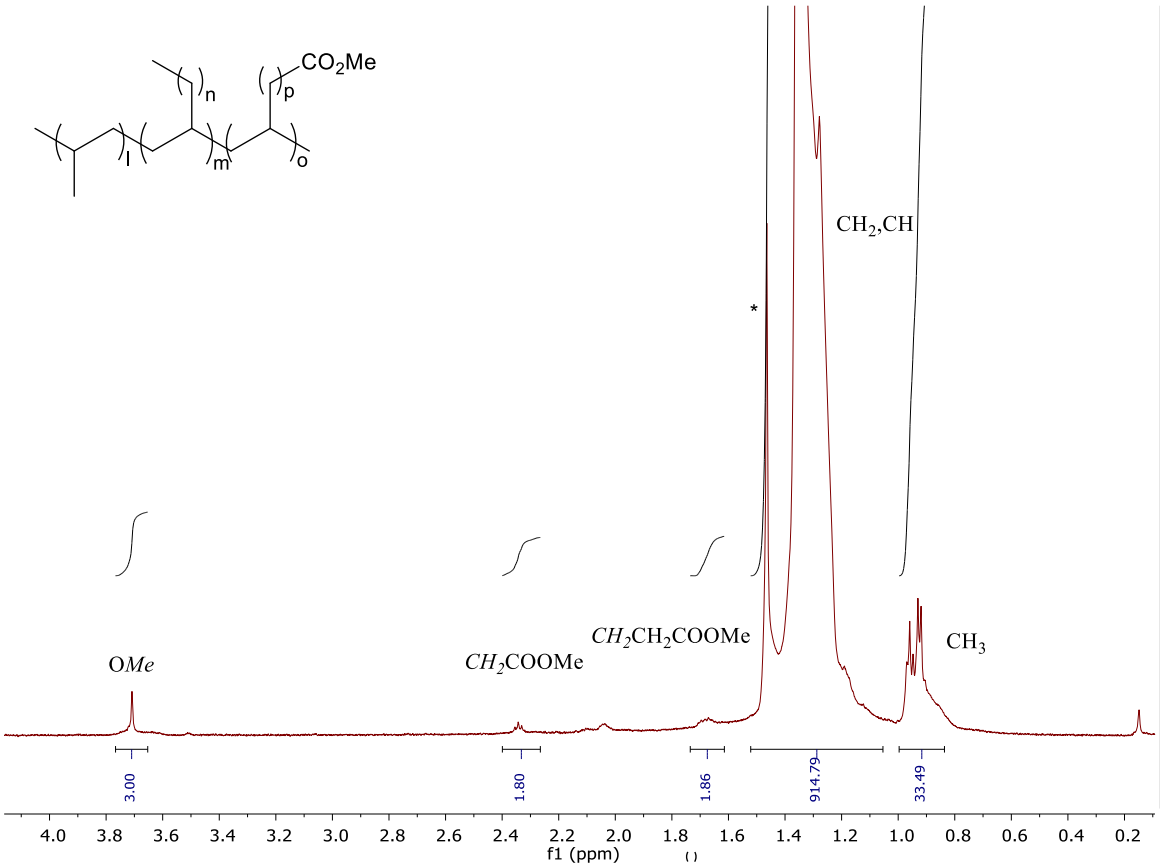

$$\text{The MA incorporation ratio (\%) =Incorporation ratio (\%)}=\frac{\frac{3}{3}}{\frac{3}{3}+\frac{914.79+33.49-2}{4}}*100=0.43\%$$

Figure S16. ^{1}H NMR analysis of the copolymer from table 1, entry 8 recorded in $C_2D_2Cl_4$ at 120 ^{o}C. *=H_2O

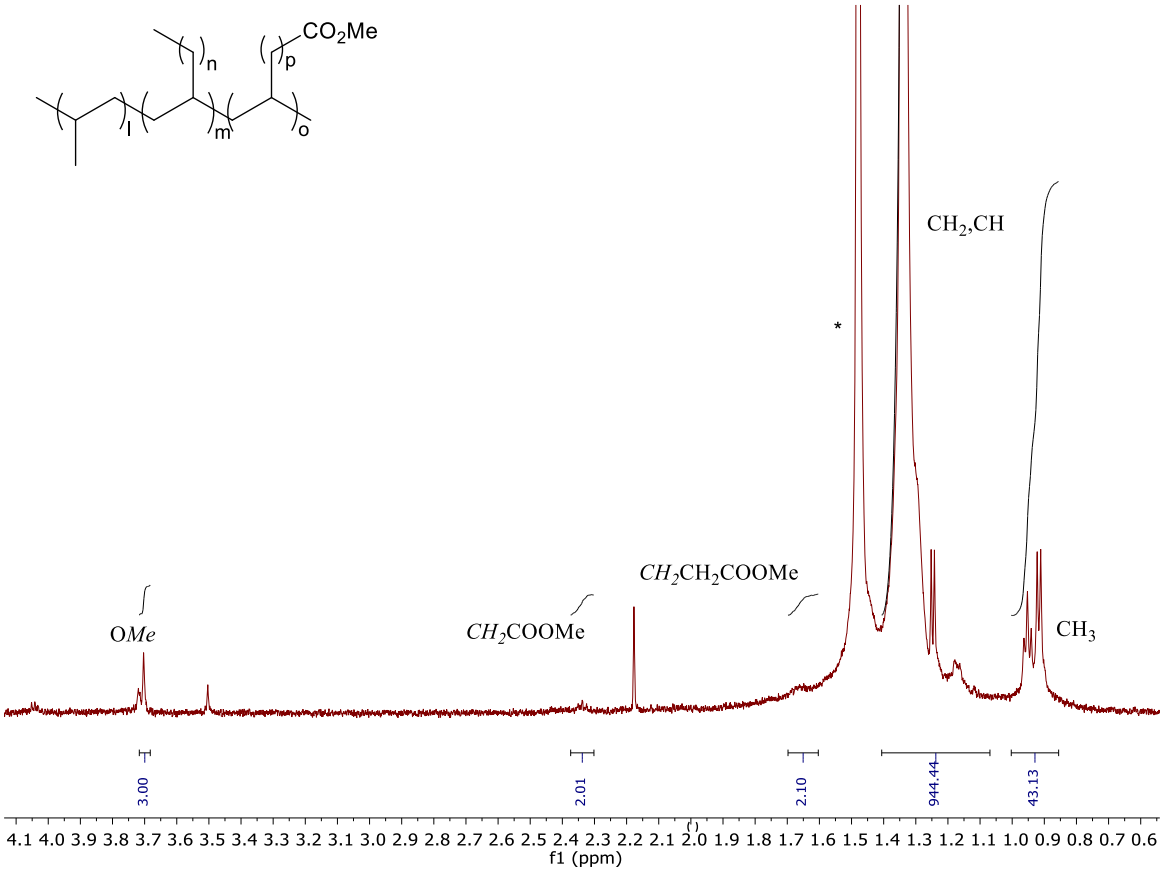

The MA incorporation ratio (%) =Incorporation ratio (%)=$\frac{\frac{3}{3}}{\frac{3}{3}+\frac{944.44+43.13-2}{4}}$*100=0.41%

Figure S17. ^{1}H NMR analysis of the copolymer from table 1, entry 9 recorded in $C_2D_2Cl_4$ at 120 ^{o}C. *=H_2O

120 ^{o}C. *=H_2O

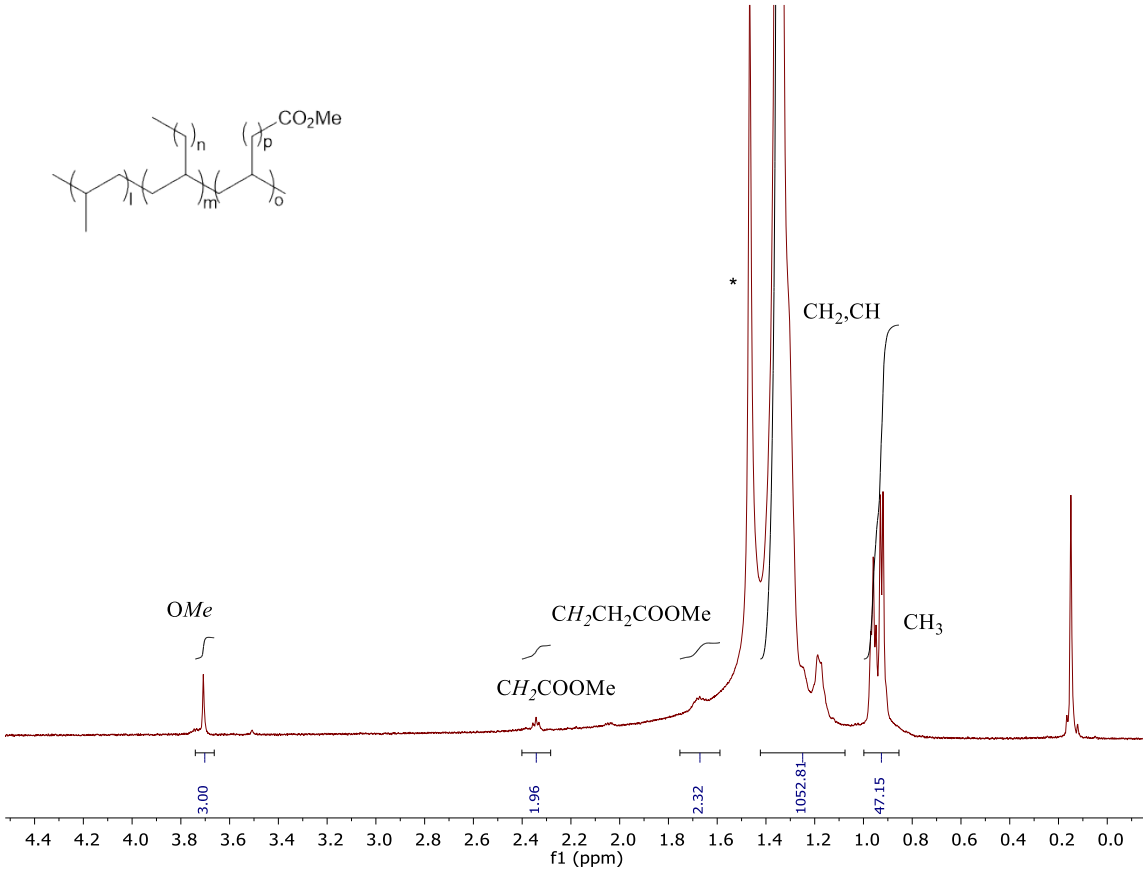

The MA incorporation ratio (%) =Incorporation ratio (%)=$\frac{\frac{3}{3}}{\frac{3}{3}+\frac{1052.81+47.15-2}{4}}$*100=0.36%

Figure S19. ^{1}H NMR analysis of the copolymer from table 1, entry 10 recorded in $C_2D_2Cl_4$ at 120 ºC. *=H_2O

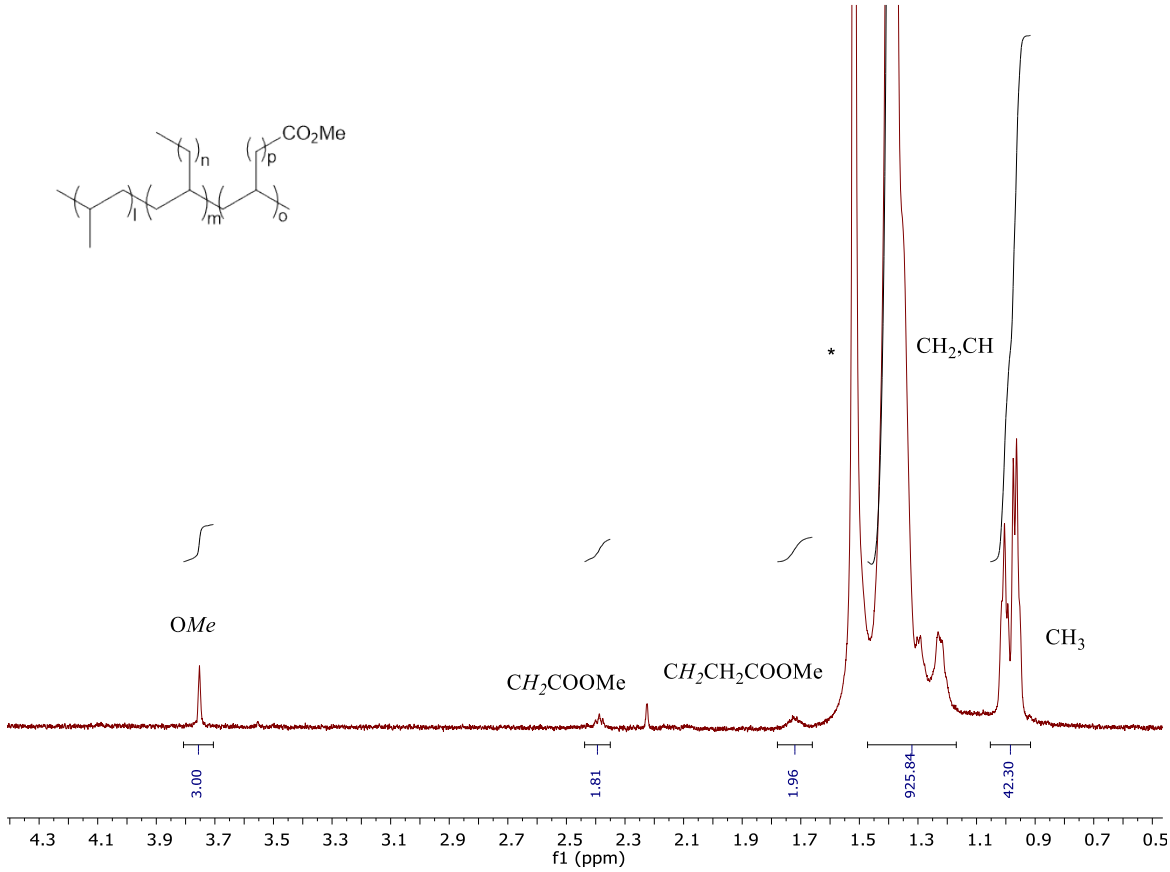

The MA incorporation ratio (%) =Incorporation ratio (%)=$\frac{\frac{3}{3}}{\frac{3}{3}+\frac{925.84+42.30-2}{4}}$*100=0.41%

Figure S20. ^{1}H NMR analysis of the copolymer from table 1, entry 11 recorded in $C_2D_2Cl_4$ at 120 ºC. *=H_2O

8. SEM of polymers and copolymers

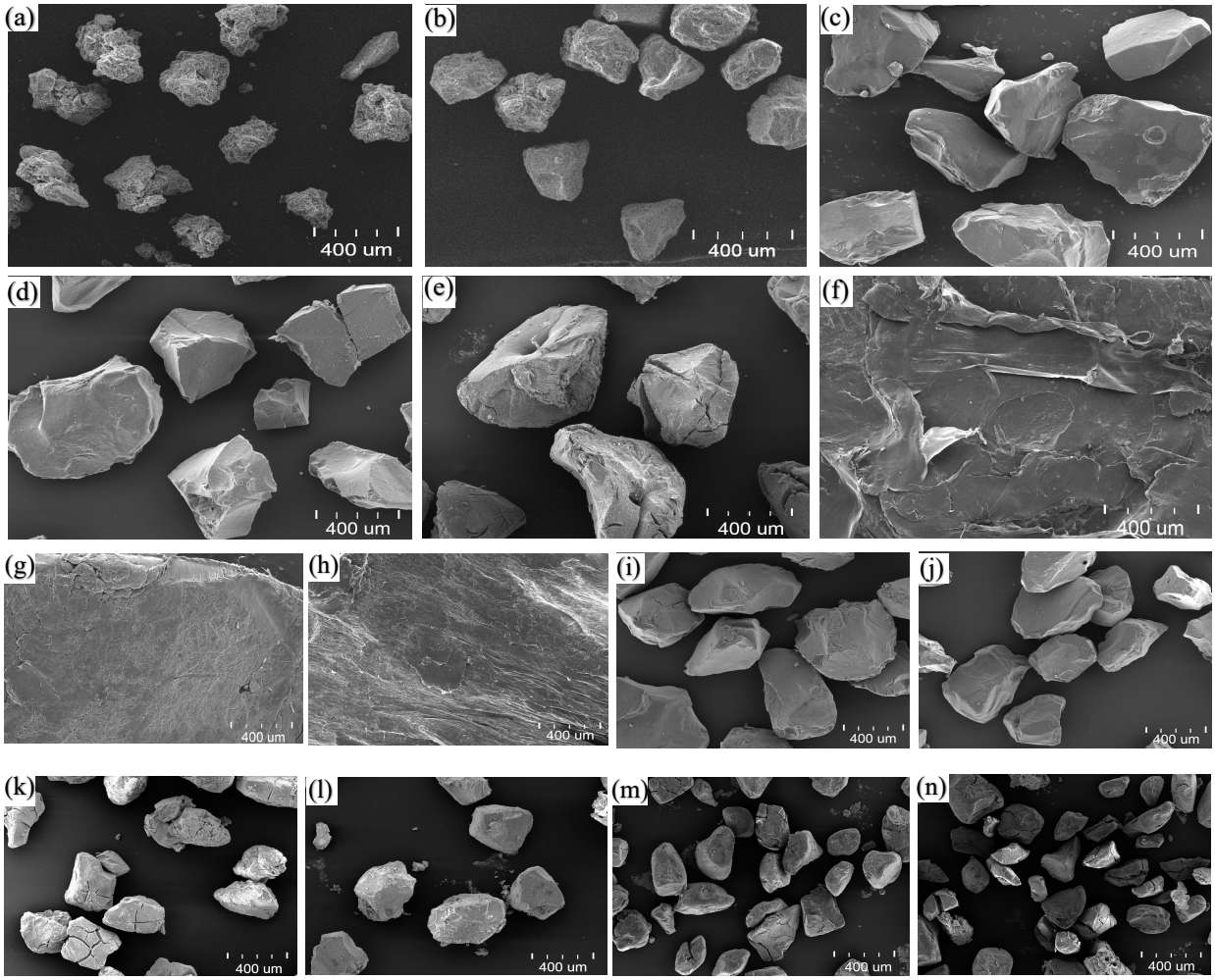

Figure S21. SEM images of polymers: a) Silica-700. b) Pd-ASO. c) table 1, entry 1. d) table 1, entry 2. e) table 1, entry 3. f) table 1, entry 4. g) table 1, entry 5. h) Polyethylene obtained using Pd/sodium tetrakis(3,5-bis(trifluoromethyl)phenyl) borate (NaBArF) at 40 °C in cyclohexane/DCM under 150 psi ethylene pressure i) table 1, entry 6. g) table 1, entry 7. k) table 1, entry 8. l) table 1, entry 9. m) table 1, entry 10. n) table 1, entry 11.

GPC of polymers and copolymers

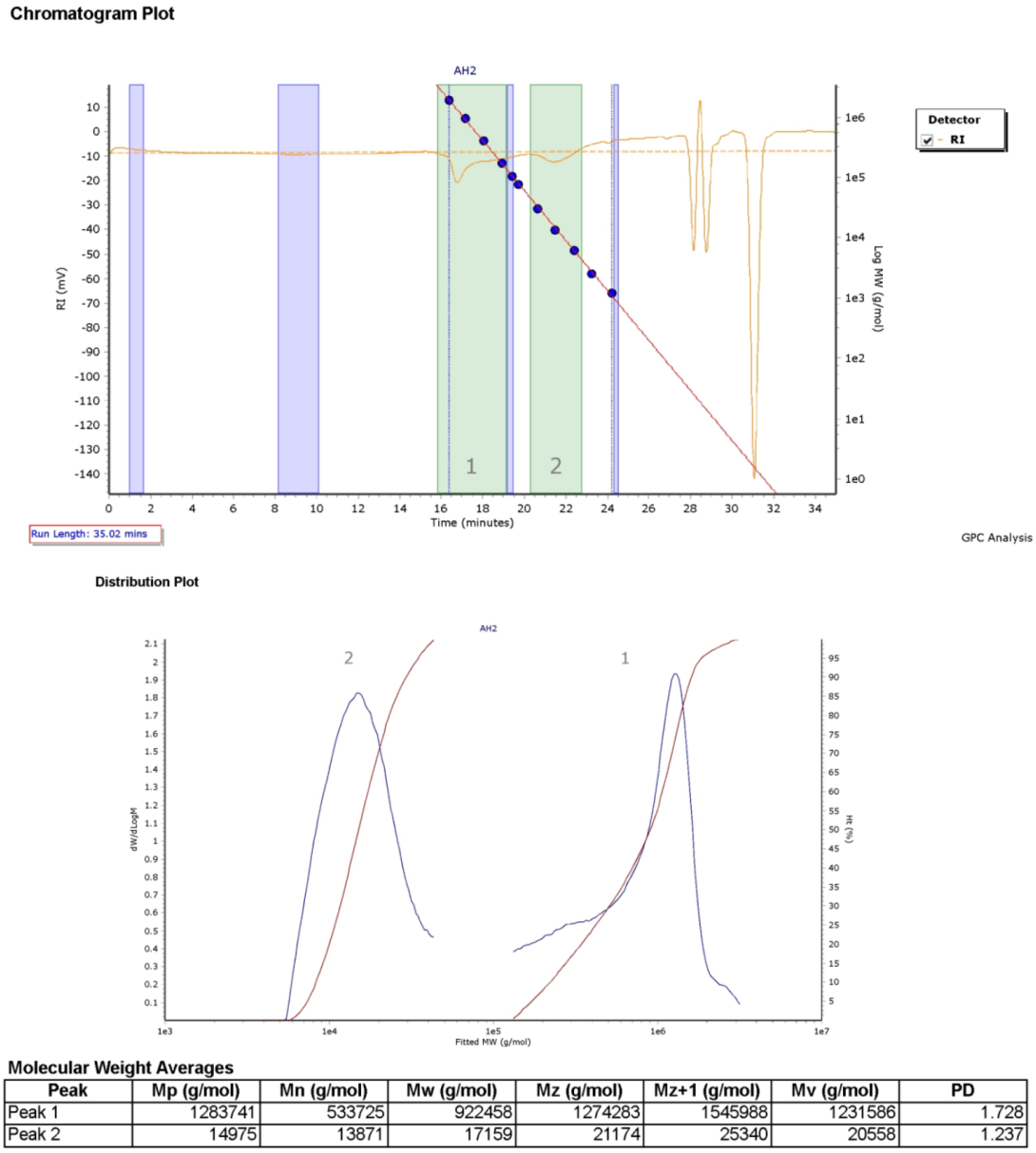

Molecular Weight Averages

Peak	Mp (g/mol)	Mn (g/mol)	Mw (g/mol)	Mz (g/mol)	Mz+1 (g/mol)	Mv (g/mol)	PD
Peak 1	1283741	533725	922458	1274283	1545988	1231586	1.728
Peak 2	14975	13871	17159	21174	25340	20558	1.237

Figure S22. GPC of the polymer from table 1, entry 1.

Chromatogram Plot

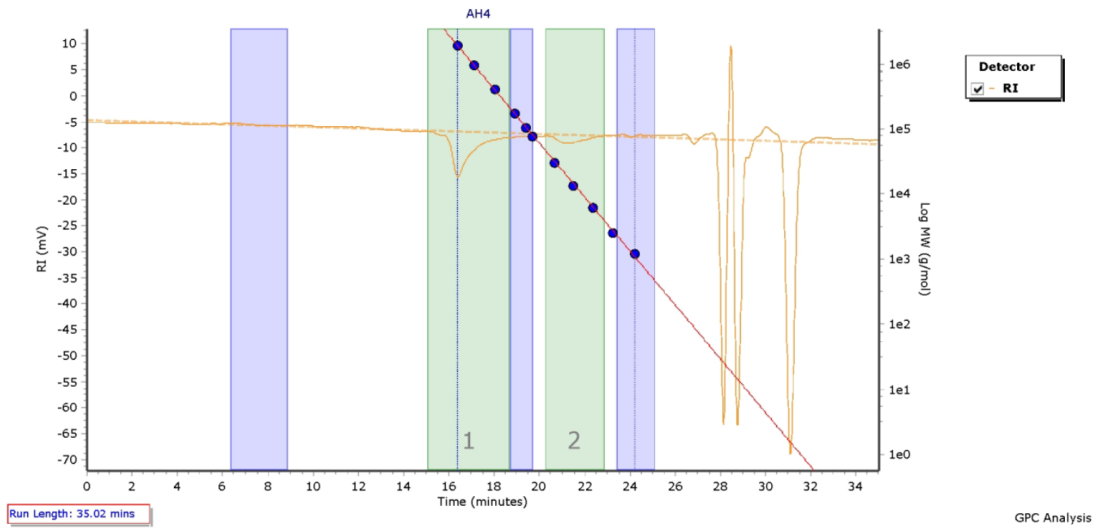

Distribution Plot

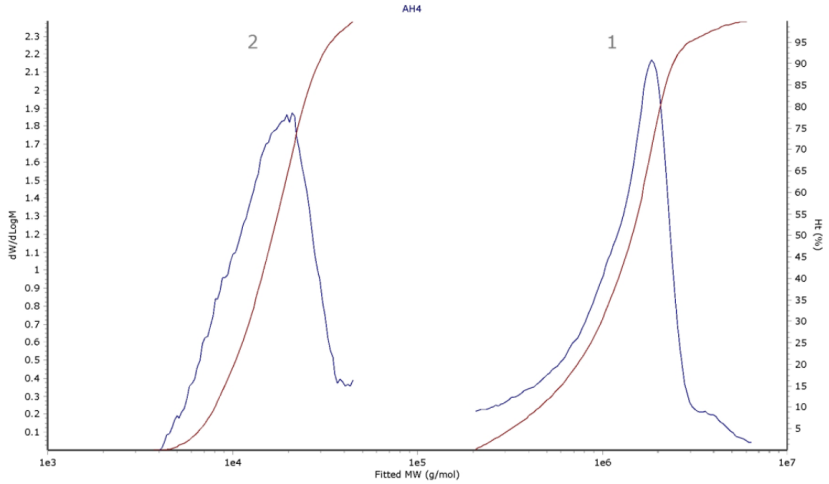

Molecular Weight Averages

Peak	Mp (g/mol)	Mn (g/mol)	Mw (g/mol)	Mz (g/mol)	Mz+1 (g/mol)	Mv (g/mol)	PD
Peak 1	1850411	971640	1501050	2021052	2588317	1944644	1.545
Peak 2	20910	14011	17736	21671	25419	21104	1.266

Figure S23. GPC of the polymer from table 1, entry 2.

Chromatogram Plot

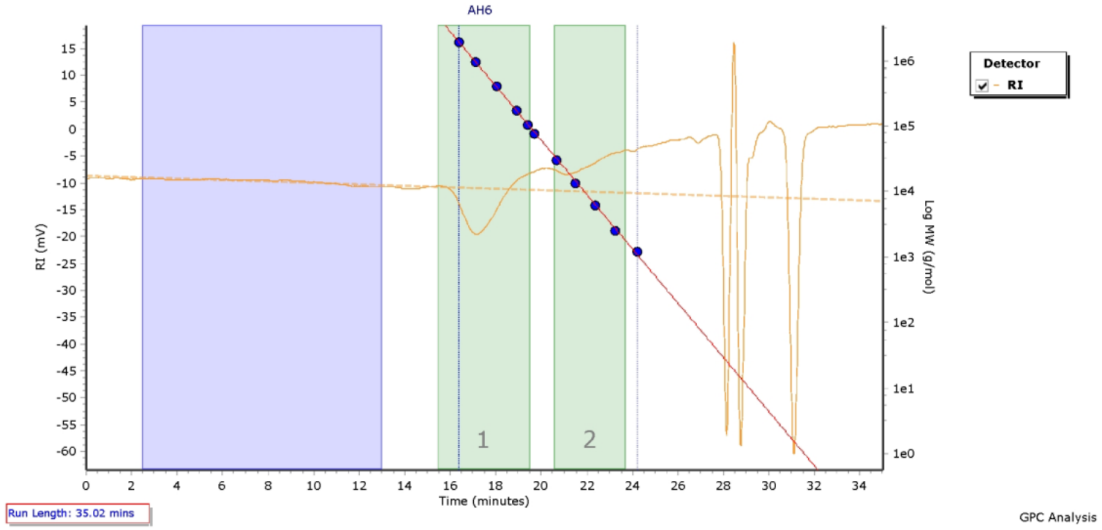

Distribution Plot

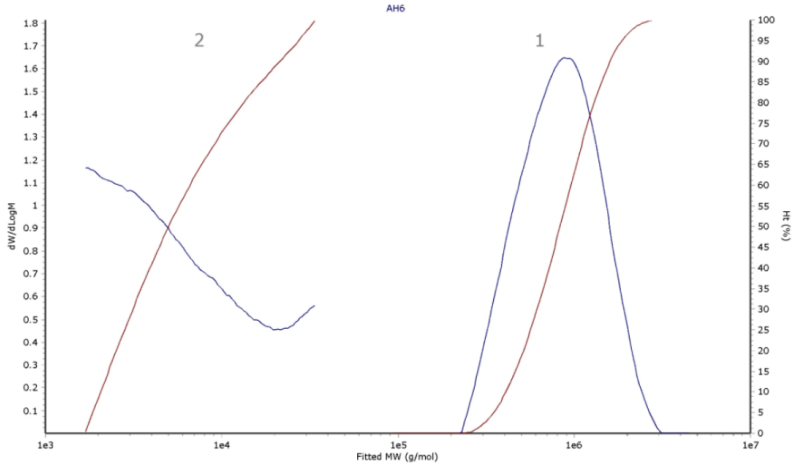

Molecular Weight Averages

Peak	Mp (g/mol)	Mn (g/mol)	Mw (g/mol)	Mz (g/mol)	Mz+1 (g/mol)	Mv (g/mol)	PD
Peak 1	876562	720731	930431	1172969	1416480	1136850	1.291
Peak 2	1724	4269	8377	15804	22008	14761	1.962

Figure S24. GPC of the polymer from table 1, entry 3.

Chromatogram Plot

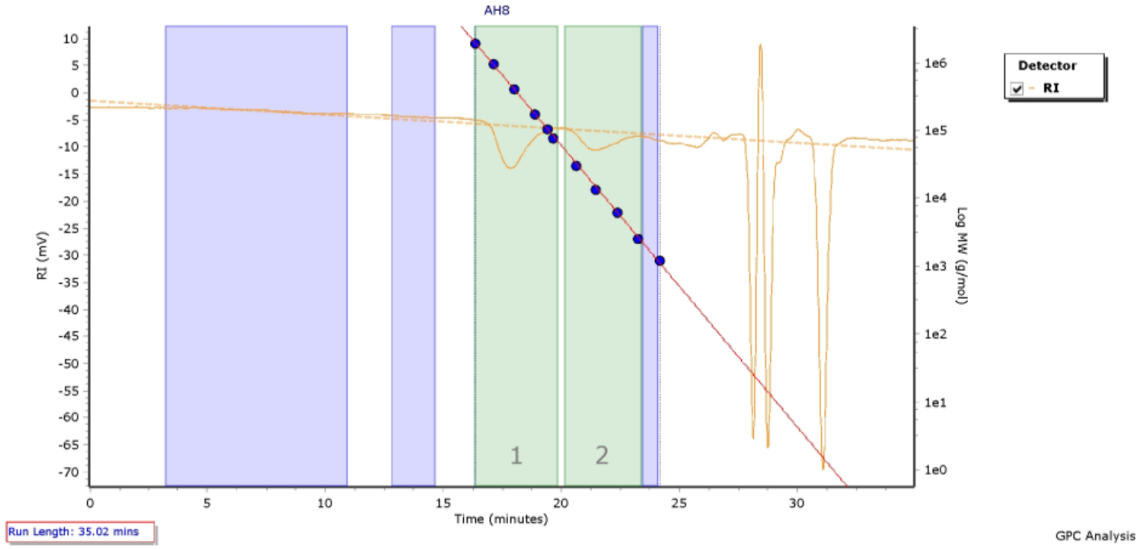

Distribution Plot

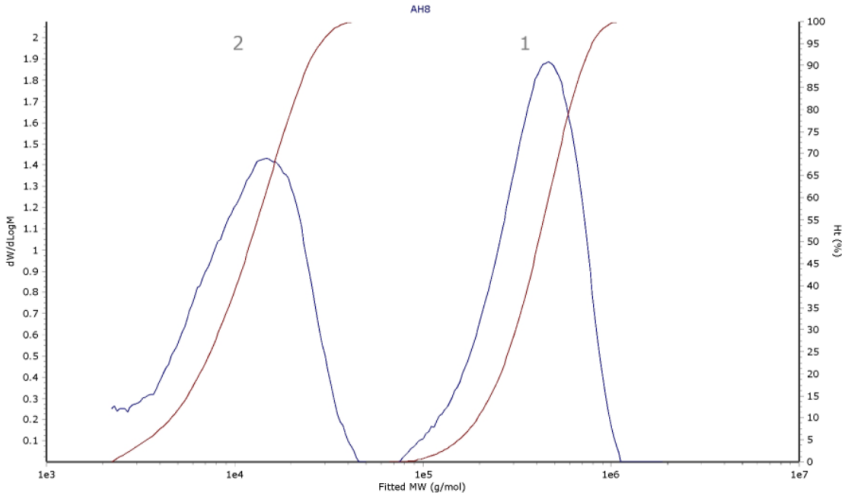

Molecular Weight Averages

Peak	Mp (g/mol)	Mn (g/mol)	Mw (g/mol)	Mz (g/mol)	Mz+1 (g/mol)	Mv (g/mol)	PD
Peak 1	471551	340587	434776	522274	597922	510411	1.277
Peak 2	14739	9127	13576	18058	21922	17455	1.487

Figure S25. GPC of the polymer from table 1, entry 4.

Chromatogram Plot

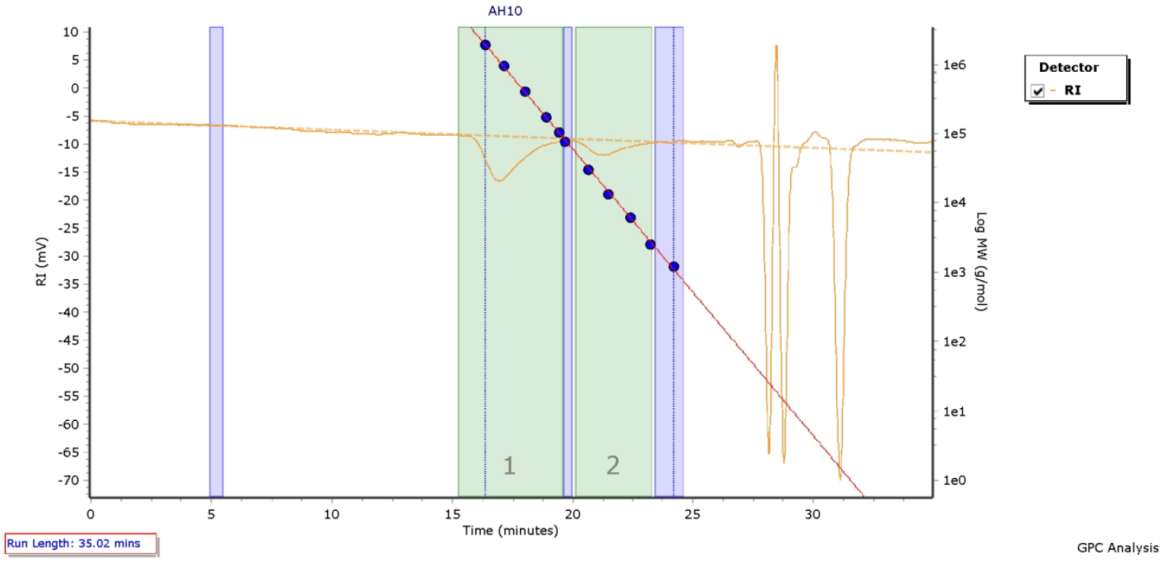

Distribution Plot

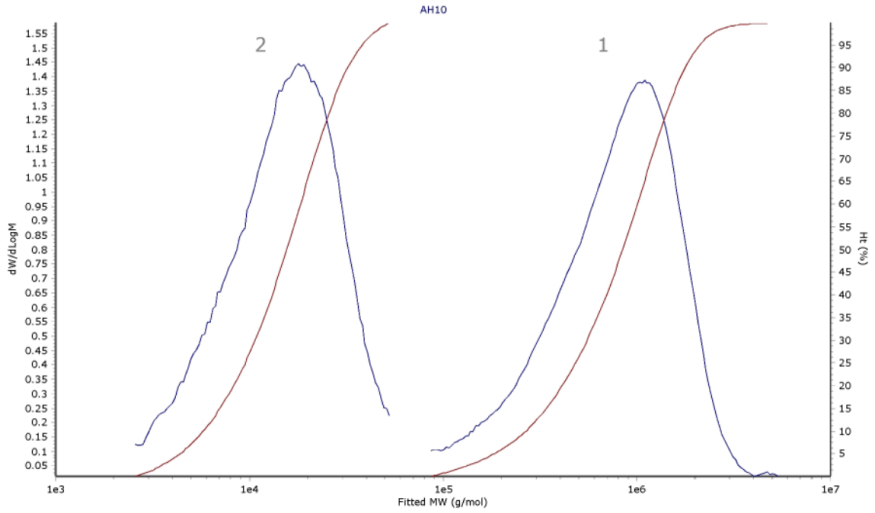

Molecular Weight Averages

Peak	Mp (g/mol)	Mn (g/mol)	Mw (g/mol)	Mz (g/mol)	Mz+1 (g/mol)	Mv (g/mol)	PD
Peak 1	1095060	557228	958755	1377039	1811102	1317145	1.721
Peak 2	17555	11611	17544	23680	29075	22844	1.511

Figure S26. GPC of the polymer from table 1, entry 5.

Chromatogram Plot

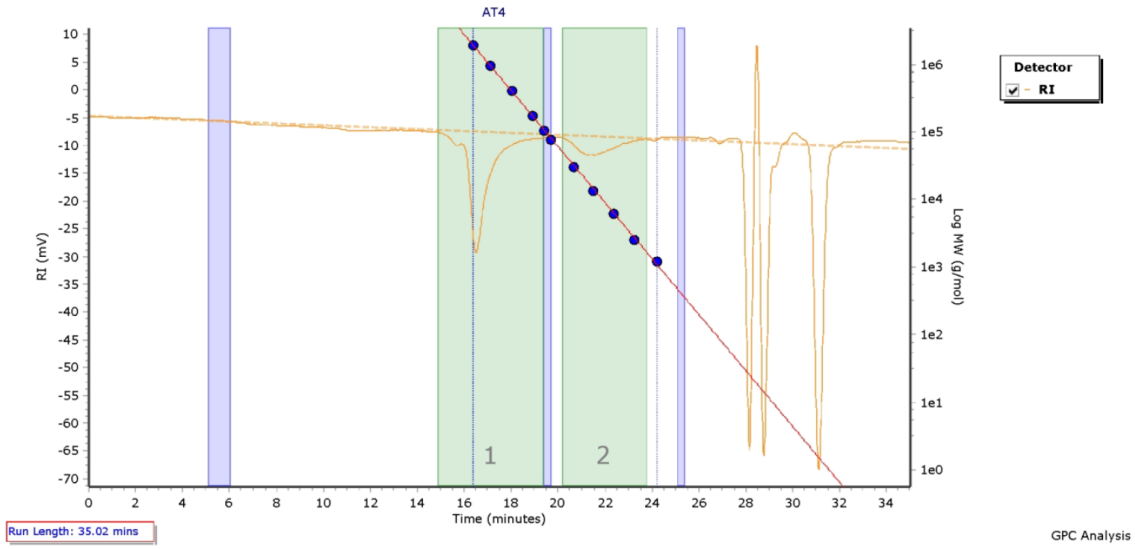

Distribution Plot

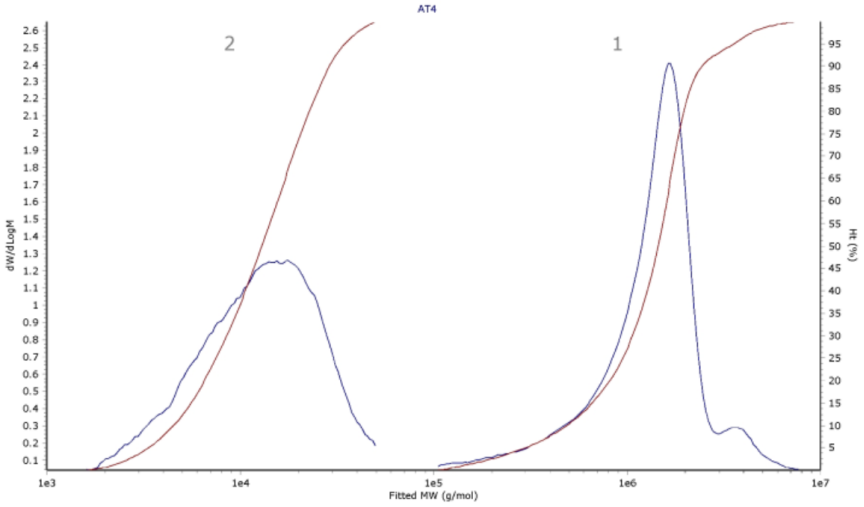

Molecular Weight Averages

Peak	Mp (g/mol)	Mn (g/mol)	Mw (g/mol)	Mz (g/mol)	Mz+1 (g/mol)	Mv (g/mol)	PD
Peak 1	1655543	928073	1547371	2191421	3057309	2084345	1.667
Peak 2	17837	9290	15155	21505	27100	20639	1.631

Figure S27. GPC of the polymer from table 1, entry 6.

Chromatogram Plot

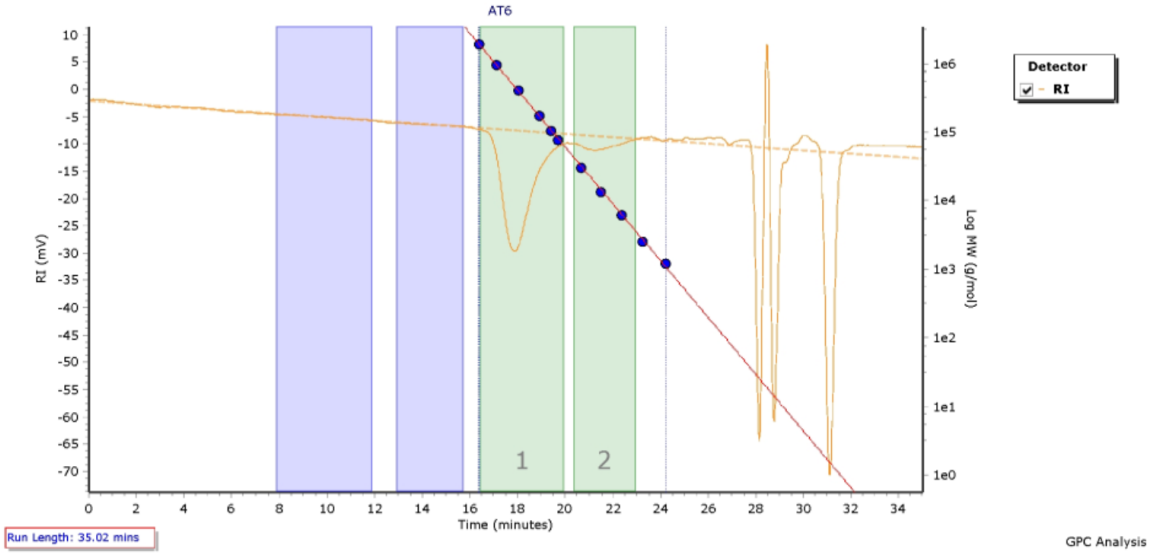

Distribution Plot

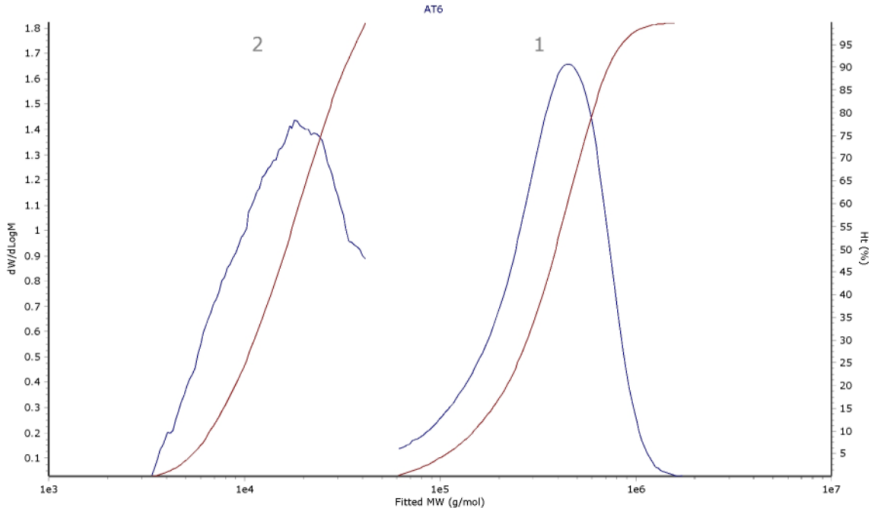

Molecular Weight Averages

Peak	Mp (g/mol)	Mn (g/mol)	Mw (g/mol)	Mz (g/mol)	Mz+1 (g/mol)	Mv (g/mol)	PD
Peak 1	449590	290405	422457	551991	678566	533694	1.455
Peak 2	18123	12914	18020	23147	27270	22473	1.395

Figure S28. GPC of the polymer from table 1, entry 7.

Chromatogram Plot

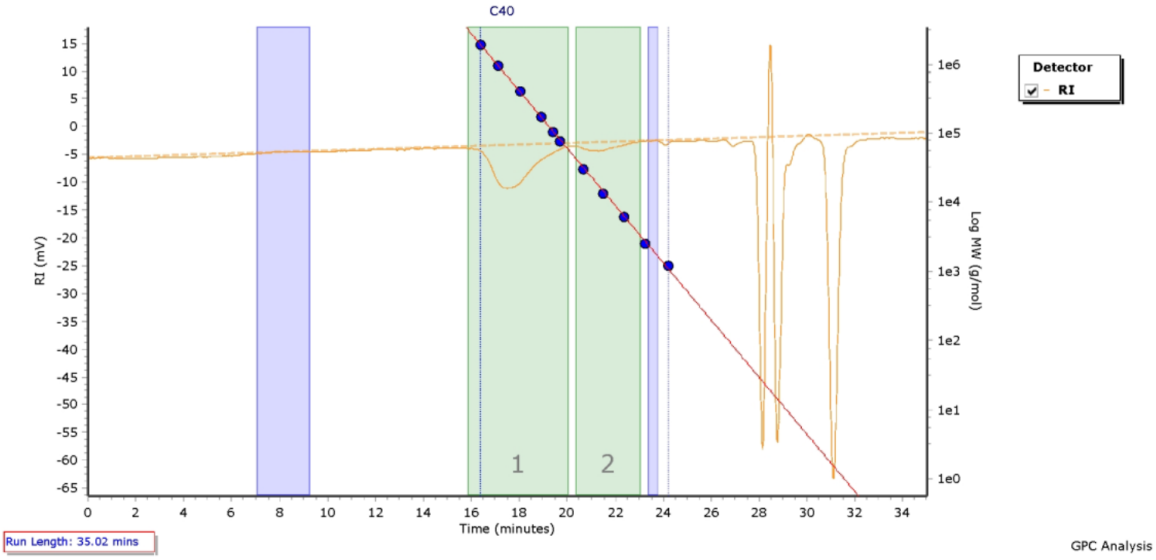

Distribution Plot

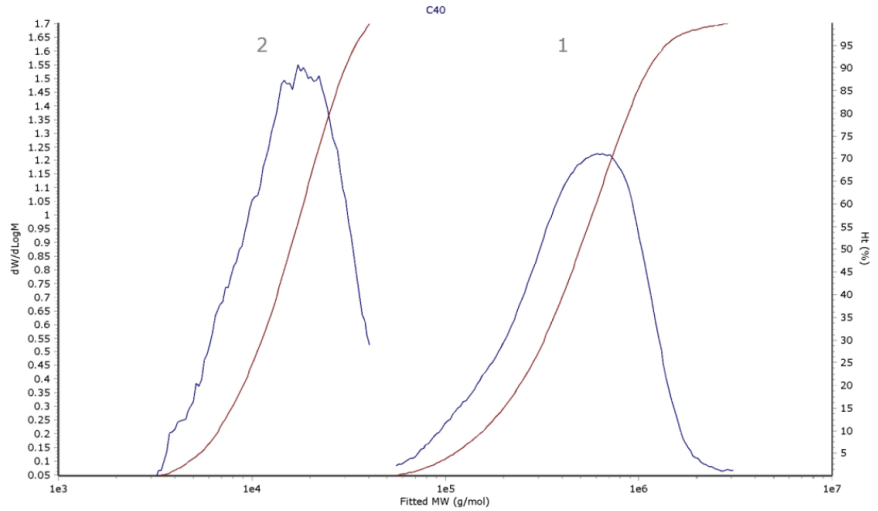

Molecular Weight Averages

Peak	Mp (g/mol)	Mn (g/mol)	Mw (g/mol)	Mz (g/mol)	Mz+1 (g/mol)	Mv (g/mol)	PD
Peak 1	648048	336450	596186	913543	1272282	865100	1.772
Peak 2	17279	12647	17282	21828	25577	21224	1.366

Figure S29. GPC of the polymer from table 1, entry 8.

Chromatogram Plot

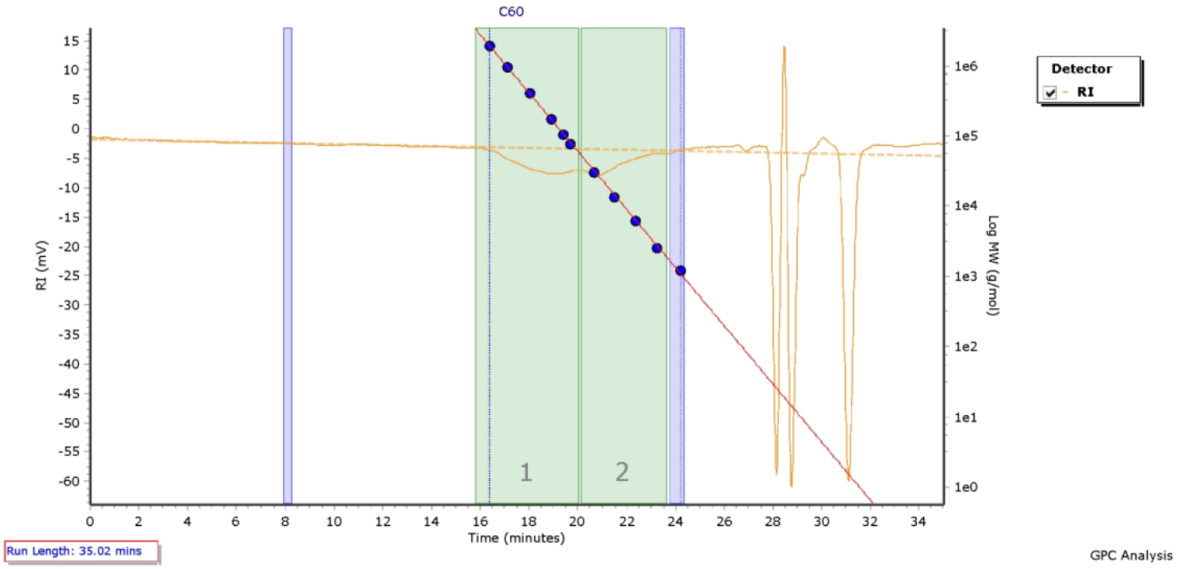

Distribution Plot

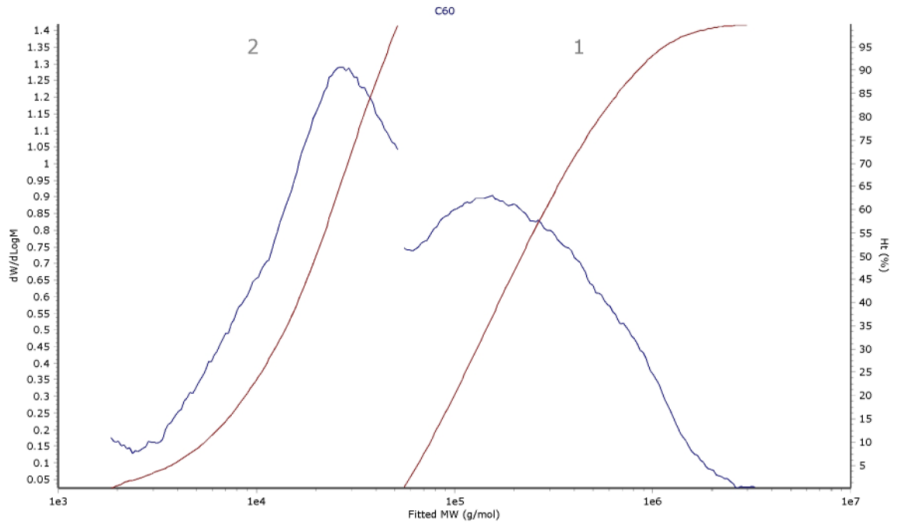

Molecular Weight Averages

Peak	Mp (g/mol)	Mn (g/mol)	Mw (g/mol)	Mz (g/mol)	Mz+1 (g/mol)	Mv (g/mol)	PD
Peak 1	154972	168022	362025	784419	1310948	713623	2.155
Peak 2	26122	12059	21912	30065	35403	29142	1.817

Figure S30. GPC of the polymer from table 1, entry 9.

Chromatogram Plot

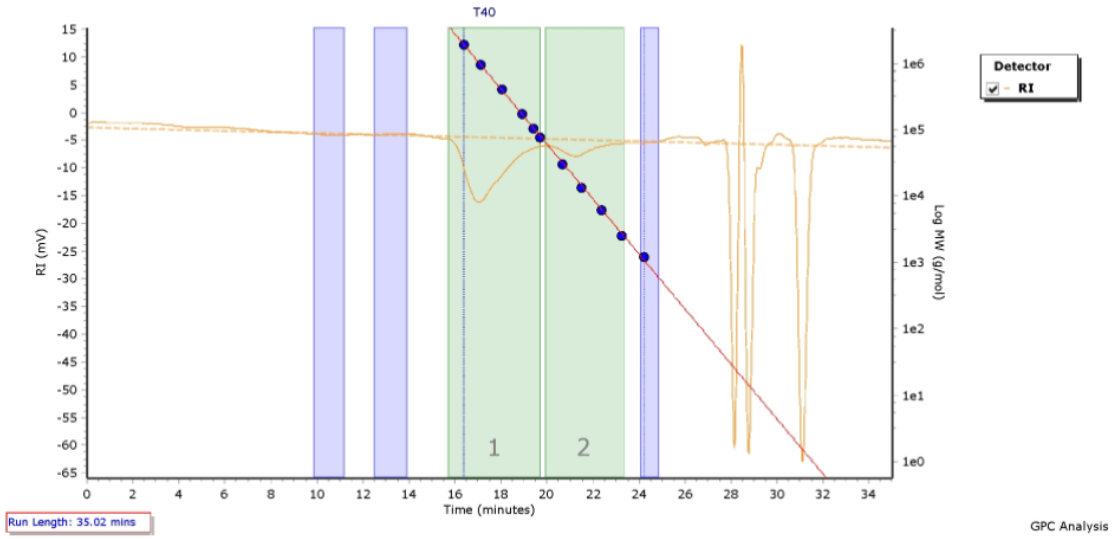

Distribution Plot

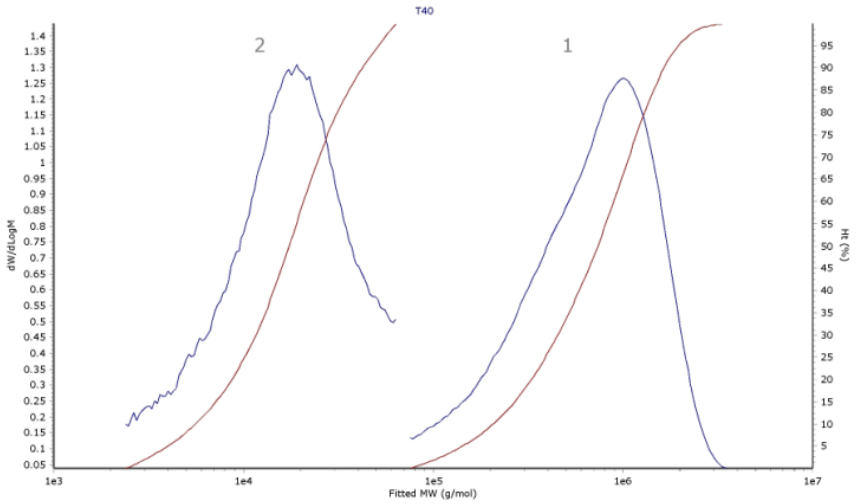

Molecular Weight Averages

Peak	Mp (g/mol)	Mn (g/mol)	Mw (g/mol)	Mz (g/mol)	Mz+1 (g/mol)	Mv (g/mol)	PD
Peak 1	1011389	459606	849839	1247038	1586299	1194999	1.849
Peak 2	19008	12090	20832	30428	38624	29135	1.723

Figure S31. GPC of the polymer from table 1, entry 10.

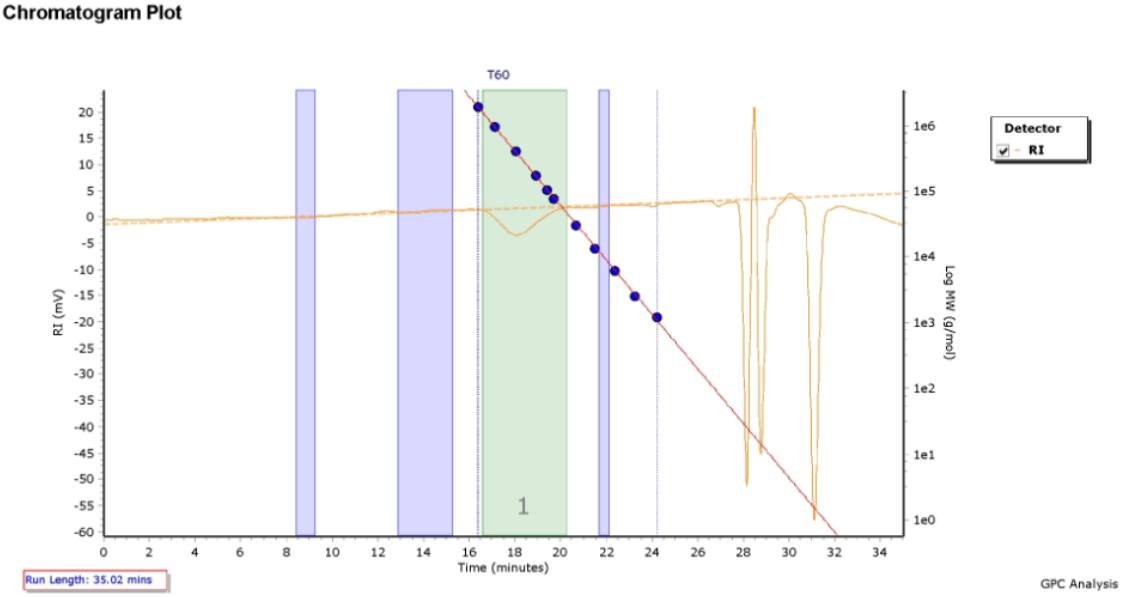

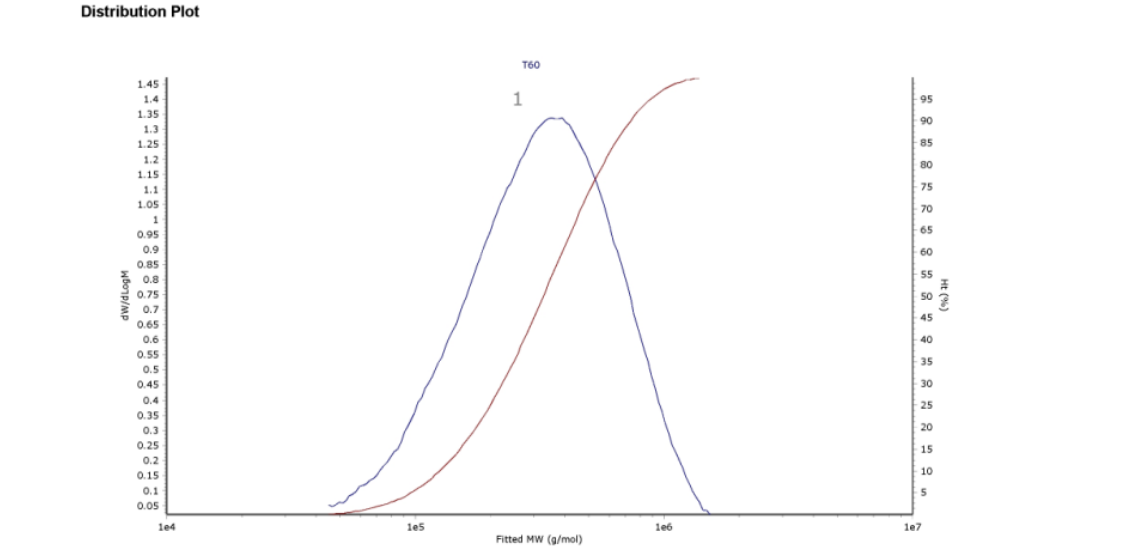

Molecular Weight Averages

Peak	Mp (g/mol)	Mn (g/mol)	Mw (g/mol)	Mz (g/mol)	Mz+1 (g/mol)	Mv (g/mol)	PD
Peak 1	354207	248042	385863	544546	697375	521724	1.556

Figure S32. GPC of the polymer from table 1, entry 11.

Fractionation of bimodal copolymer

200 mg copolymer from Table 1 Entry 8 was suspended in toluene (50 mL) containing 2,6-bis(1,1-dimethylethyl)-4-methylphenol (BHT, 40 mg) and heated to 140 °C for 1 h. Silica separated from the solution and was removed by vacuum filtration. The transparent hot toluene solution was cooled to 120 °C and ethylene glycol (40 mL) was added dropwise. The mixture was maintained at 120 °C for 3h. The polymer precipitate that forms over this time was filtered away to yield 16 mg of material, and is referred to as "fraction 1." The resulting toluene solution was cooled to room temperature, methanol (100 mL) was added to precipitate polymer to give 52 mg of material, and is referred to as "fraction 2." Fraction 2 was re-dissolved in toluene (50 mL) at 140°C for 1 h and cooled down to room temperature. The precipitated polymer was filtered away, and the clar toluene solution containing the lowest molecular weight fraction was treated with methanol (50 mL) to give 18 mg of materials, and is referred to as "fraction 3."

Table S4. Fraction data of bimodal copolymer (table 1, entry 8)

	$X^{[a]}$	$M_n^{[b]}$ (kg/mol)
Entry 8, fraction 1	0.47	1437
Entry 8, fraction 2	0.39	376
Entry 8, fraction 3	0.40	98.4[c]

[a] Incorporation of methyl acrylate into the co-polymer determined by ^{1}H NMR in tetrachloroethane-d_2 at 120 °C. [b] Determined by GPC in trichlorobenzene at 150 °C. [c] Determined by ^{1}H NMR in $C_2D_2Cl_4$ at 120 °C.

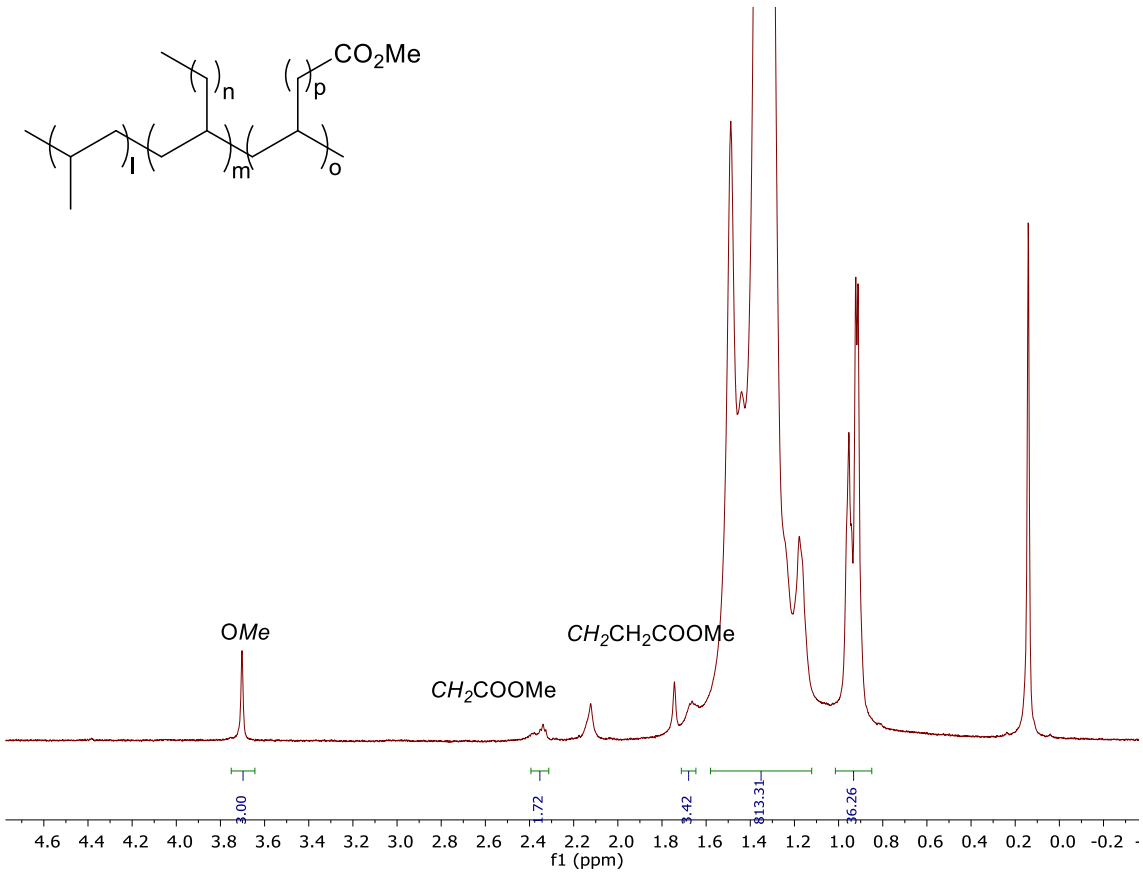

Figure S33. ^{1}H NMR analysis of the table S4, fraction 1.

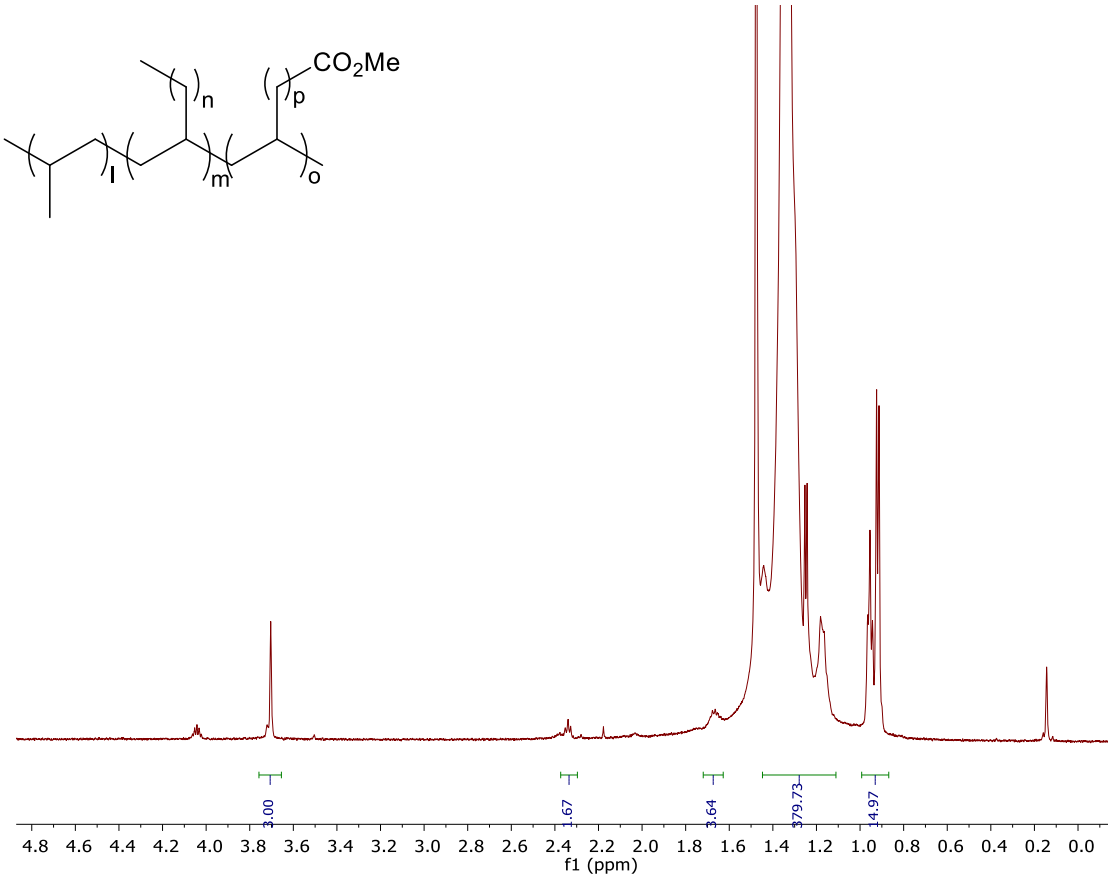

Figure S34. ^{1}H NMR analysis of the table S4, fraction 2.

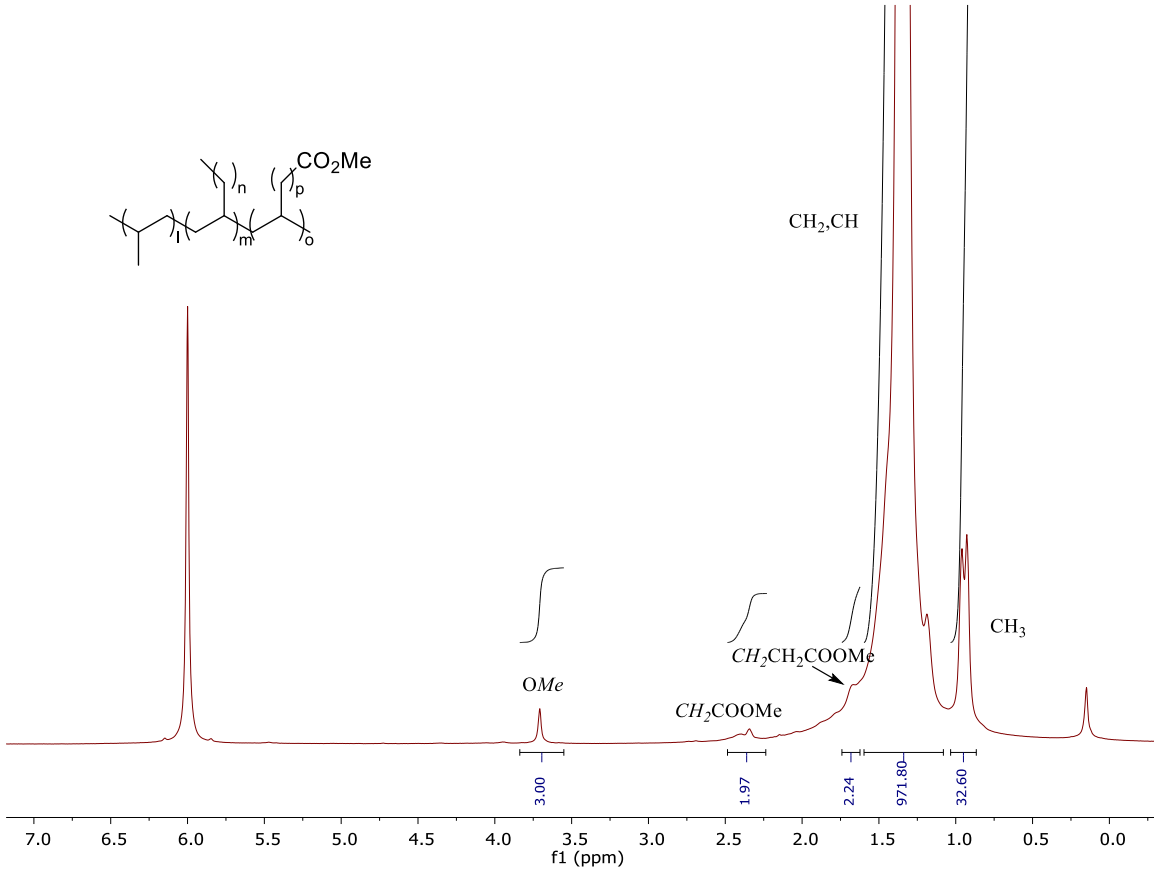

Figure S35. ^{1}H NMR analysis of the table S4, fraction 3.

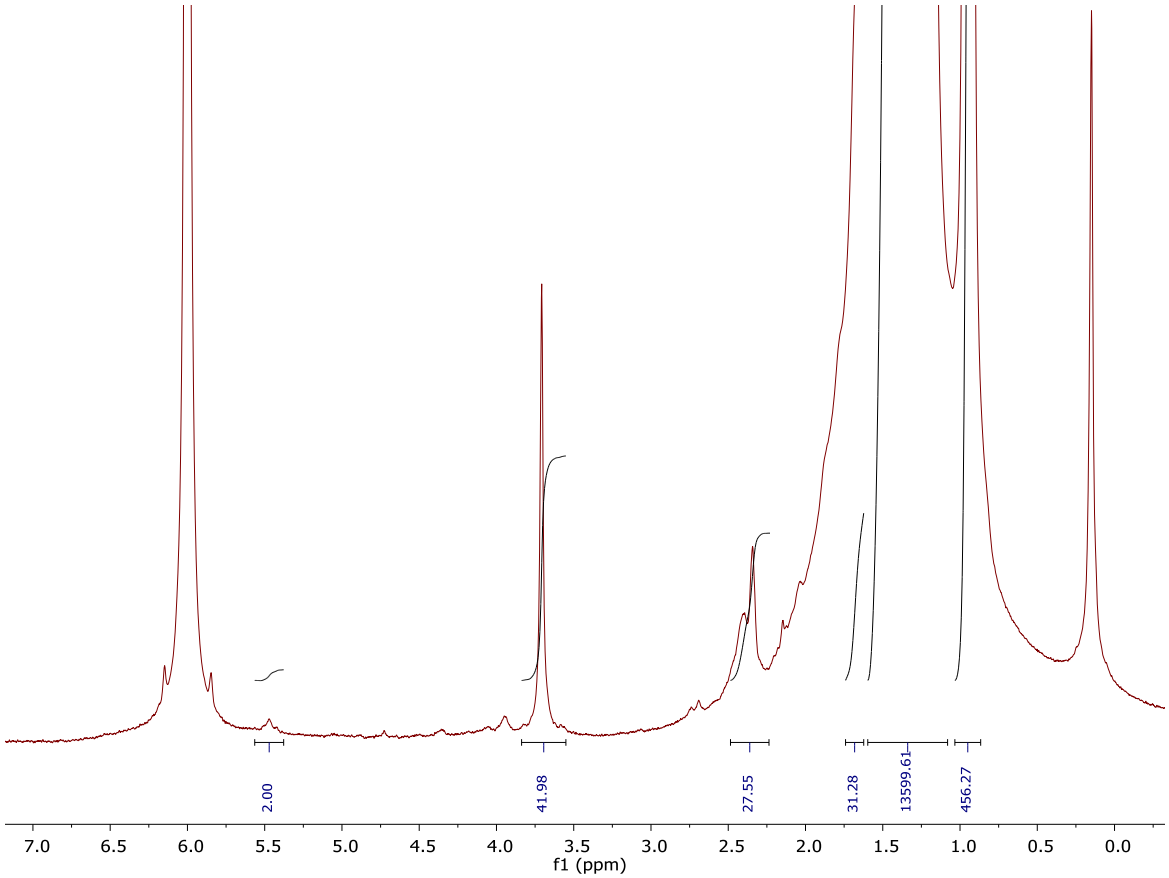

The molecular weight of the low fraction of polyethylene was calculated from ^{1}H NMR[12]

$$M_n = \frac{\frac{I_{tot}}{4}}{\left(\frac{I_2}{2}\right)} * 28 = M_n = \frac{\frac{2+13599.61+456.27}{4}}{\left(\frac{2}{2}\right)} * 28 = 98405$$

Figure S36. Expansion of the ^{1}H NMR spectrum of fraction 3 showing internal olefin signals, and calculation of M_n from this NMR data.

Chromatogram Plot

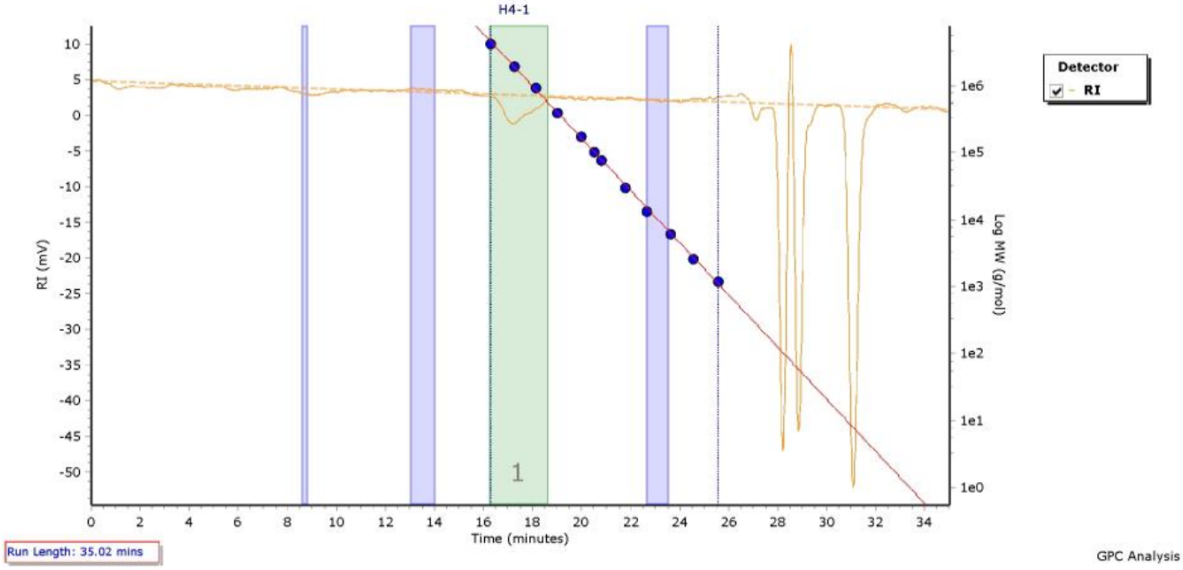

Distribution Plot

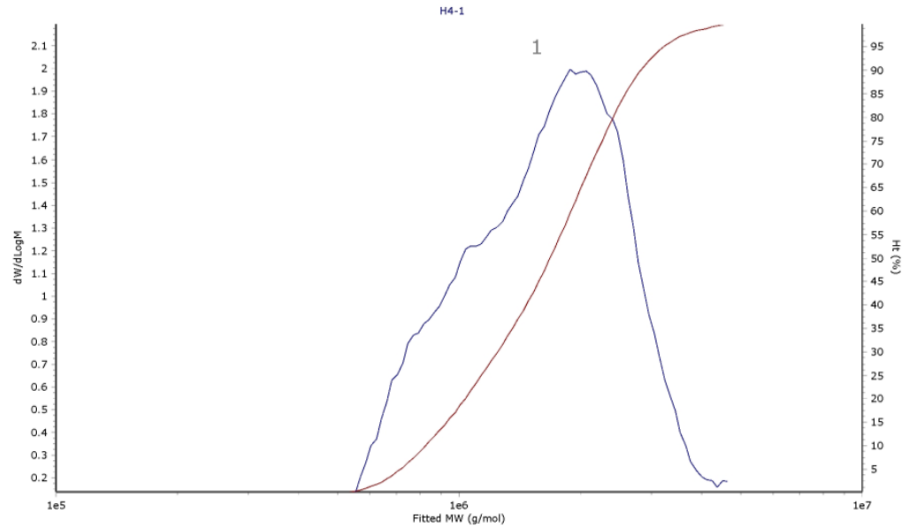

Molecular Weight Averages

Peak	Mp (g/mol)	Mn (g/mol)	Mw (g/mol)	Mz (g/mol)	Mz+1 (g/mol)	Mv (g/mol)	PD
Peak 1	1888565	1437433	1771547	2121427	2453689	2071148	1.232

Figure S37. GPC of the polymer from table S3, fraction 1

Chromatogram Plot

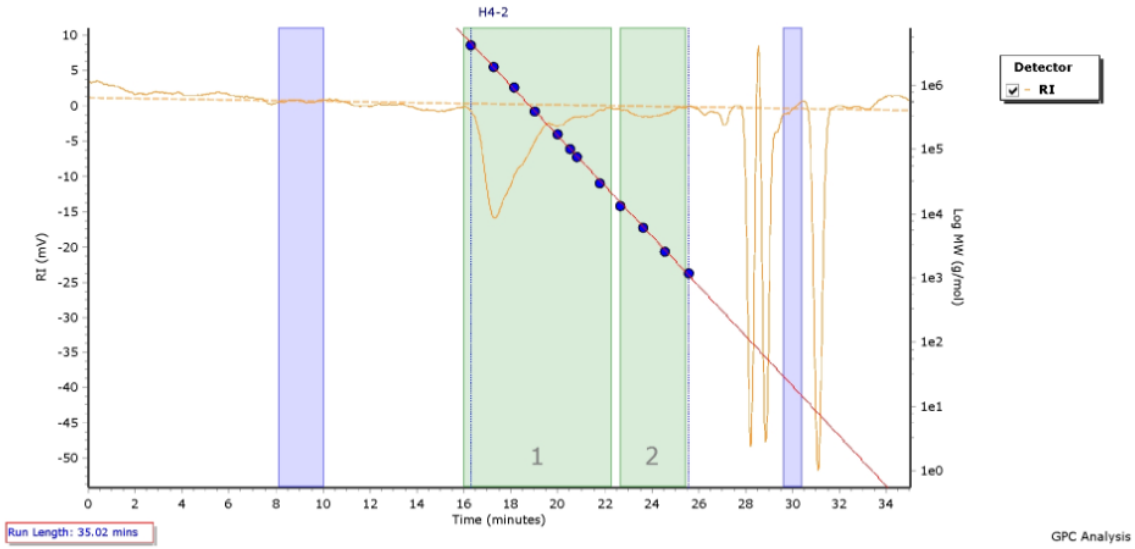

Distribution Plot

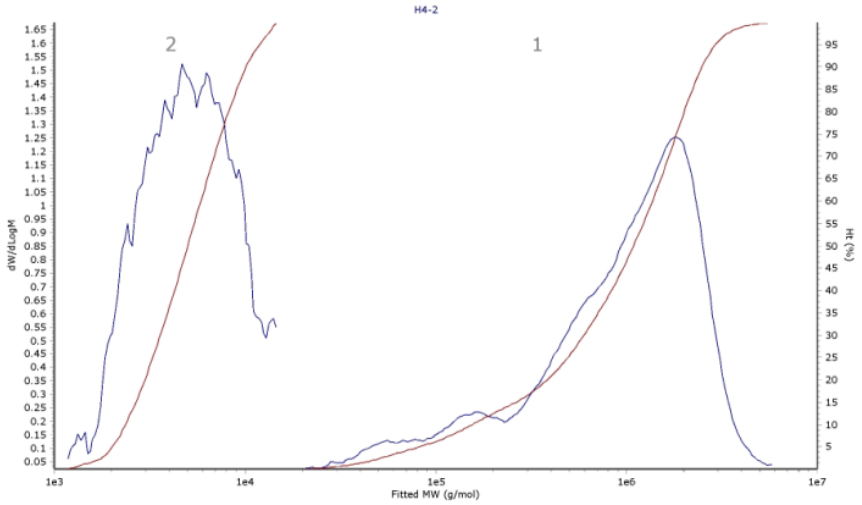

Molecular Weight Averages

Peak	Mp (g/mol)	Mn (g/mol)	Mw (g/mol)	Mz (g/mol)	Mz+1 (g/mol)	Mv (g/mol)	PD
Peak 1	1805630	376219	1246563	1948252	2474285	1867538	3.313
Peak 2	4669	4254	5694	7311	8798	7080	1.339

Figure S38. GPC of the polymer from table S3, fraction 2

References

(1) aRhinehart, J. L.; Brown, L. A.; Long, B. K. A Robust Ni(II) α-Diimine Catalyst for High Temperature Ethylene Polymerization. *J. Am. Chem. Soc.* **2013**, *135*, 16316-16319; bDai, S.; Sui, X.; Chen, C. Highly Robust Palladium(II) α-Diimine Catalysts for Slow-Chain-Walking Polymerization of Ethylene and Copolymerization with Methyl Acrylate. *Angew. Chem., Int. Ed.* **2015**, *54*, 9948-9953; cDai, S.; Chen, C. Direct Synthesis of Functionalized High-Molecular-Weight Polyethylene by Copolymerization of Ethylene with Polar Monomers. *Angewandte Chemie International Edition* **2016**, *55*, 13281-13285.

(2) Müller, L. O.; Himmel, D.; Stauffer, J.; Steinfeld, G.; Slattery, J.; Santiso-Quiñones, G.; Brecht, V.; Krossing, I. Simple Access to the Non-Oxidizing Lewis Superacid PhF→Al(ORF)3 (RF=C(CF3)3). *Angew. Chem., Int. Ed.* **2008**, *47*, 7659-7663.

(3) Culver, D. B.; Venkatesh, A.; Huynh, W.; Rossini, A. J.; Conley, M. P. Al(ORF)3 (RF = C(CF3)3) activated silica: a well-defined weakly coordinating surface anion. *Chem. Sci.* **2020**, *11*, 1510 - 1517.

(4) Harris, R. K.; Becker, E. D.; Cabral de Menezes, S. M.; Goodfellow, R.; Granger, P. NMR Nomenclature: Nuclear Spin Properties and Conventions for Chemical Shifts: IUPAC Recommendations 2001. *Solid State Nucl. Magn. Reson.* **2002**, *22*, 458-483.

(5) Brinkmann, A.; Kentgens, A. P. M. Proton-Selective 17O−H Distance Measurements in Fast Magic-Angle-Spinning Solid-State NMR Spectroscopy for the Determination of Hydrogen Bond Lengths. *J. Am. Chem. Soc.* **2006**, *128*, 14758-14759.

(6) aPourpoint, F.; Trebosc, J.; Gauvin, R. M.; Wang, Q.; Lafon, O.; Deng, F.; Amoureux, J.-P. Measurement of aluminum-carbon distances using S-RESPDOR NMR experiments. *Chemphyschem : a European journal of chemical physics and physical chemistry* **2012**, *13 16*, 3605-3615; bNimerovsky, E.; Gupta, R.; Yehl, J.; Li, M.; Polenova, T.; Goldbourt, A. Phase-modulated LA-REDOR: A robust, accurate and efficient solid-state NMR technique for distance measurements between a spin-1/2 and a quadrupole spin. *J. Magn. Reson.* **2014**, *244*, 107-113.

(7) Fung, B. M.; Khitrin, A. K.; Ermolaev, K. An Improved Broadband Decoupling Sequence for Liquid Crystals and Solids. *J. Magn. Reson.* **2000**, *142*, 97-101.

(8) aChan, J. C. C.; Eckert, H. Dipolar Coupling Information in Multispin Systems: Application of a Compensated REDOR NMR Approach to Inorganic Phosphates. *J. Magn. Reson.* **2000**, *147*, 170-178; bBertmer, M.; Eckert, H. Dephasing of spin echoes by multiple heteronuclear dipolar interactions in rotational echo double resonance NMR experiments. *Solid State Nucl. Magn. Reson.* **1999**, *15*, 139-152; cBertmer, M.; Züchner, L.; Chan, J. C. C.; Eckert, H. Short and Medium Range Order in Sodium Aluminoborate Glasses. 2. Site Connectivities and Cation Distributions Studied by Rotational Echo Double Resonance NMR Spectroscopy. *J. Phys. Chem. B* **2000**, *104*, 6541-6553; dStrojek, W.; Kalwei, M.; Eckert, H. Dipolar NMR Strategies for Multispin Systems Involving Quadrupolar Nuclei: 31P{23Na} Rotational Echo Double Resonance (REDOR) of Crystalline Sodium Phosphates and Phosphate Glasses. *J. Phys. Chem. B* **2004**, *108*, 7061-7073; eStrojek, W.; Eckert, H. Medium-range order in sodium phosphate glasses: A quantitative rotational echo double resonance solid state NMR study. *Phys. Chem. Chem. Phys.* **2006**, *8*, 2276-2285; fHuang, S.-J.; Liu, S.-B.; Chan, J. C. C. Heteronuclear dipolar recoupling of half-integer quadrupole nuclei under fast magic angle spinning. *Solid State Nucl. Magn. Reson.* **2009**, *36*, 110-117; gAkopov, G.; Mark, J.; Viswanathan, G.; Lee, S. J.; McBride, B. C.; Won, J.; Perras, F. A.; Paterson, A. L.; Yuan, B.; Sen, S.; Adeyemi, A. N.; Zhang, F.; Wang, C.-Z.; Ho, K.-M.; Miller, G. J.; Kovnir, K. Third time's the charm: intricate non-centrosymmetric

polymorphism in LnSiP3 (Ln = La and Ce) induced by distortions of phosphorus square layers. *Dalton Trans.* **2021**, *50*, 6463-6476.

(9) Hanwell, M. D.; Curtis, D. E.; Lonie, D. C.; Vandermeersch, T.; Zurek, E.; Hutchison, G. R. Avogadro: an advanced semantic chemical editor, visualization, and analysis platform. *Journal of Cheminformatics* **2012**, *4*, 17.

(10) Sarioğlan, S. Recovery of palladium from spent activated carbon-supported palladium catalysts. . *Platin. Met. Rev.* **2013**, *57*, 289-296.

(11) Guironnet, D.; Roesle, P.; Rünzi, T.; Göttker-Schnetmann, I.; Mecking, S. Insertion Polymerization of Acrylate. *J. Am. Chem. Soc.* **2009**, *131*, 422-423.

(12) Wiedemann, T.; Voit, G.; Tchernook, A.; Roesle, P.; Göttker-Schnetmann, I.; Mecking, S. Monofunctional Hyperbranched Ethylene Oligomers. *J. Am. Chem. Soc.* **2014**, *136*, 2078-2085.